Title

The use of 7T MRI in multiple sclerosis: review and consensus statement from the North American Imaging in Multiple Sclerosis Cooperative.

Journal

Brain Communications, 6(5)

Authors

Harrison, Daniel
Sati, Pascal
Klawiter, Eric
et al.

Publication Date

2024

DOI

10.1093/braincomms/fcae359

Peer reviewed

BRAIN COMMUNICATIONS

REVIEW ARTICLE

The use of 7T MRI in multiple sclerosis: review and consensus statement from the North American Imaging in Multiple Sclerosis Cooperative

Daniel M. Harrison,[1,2] Pascal Sati,[3] Eric C. Klawiter,[4] Sridar Narayanan,[5,6] Francesca Bagnato,[7,8] Erin S. Beck,[9] Peter Barker,[10] Alberto Calvi,[11] Alessandro Cagol,[12,13,14] Maxime Donadieu,[15] Jeff Duyn,[16] Cristina Granziera,[12,13,17] Roland G. Henry,[18] Susie Y. Huang,[19] Michael N. Hoff,[20] Caterina Mainero,[19] Daniel Ontaneda,[21] Daniel S. Reich,[15] David A. Rudko,[5,22] Seth A. Smith,[23,24] Siegfried Trattnig,[25] Jonathan Zurawski,[26] Rohit Bakshi,[26] Susan Gauthier[27] and Cornelia Laule[28]; on behalf of the NAIMS Cooperative

The use of ultra-high-field 7-Tesla (7T) MRI in multiple sclerosis (MS) research has grown significantly over the past two decades. With recent regulatory approvals of 7T scanners for clinical use in 2017 and 2020, the use of this technology for routine care is poised to continue to increase in the coming years. In this context, the North American Imaging in MS Cooperative (NAIMS) convened a workshop in February 2023 to review the previous and current use of 7T technology for MS research and potential future research and clinical applications. In this workshop, experts were tasked with reviewing the current literature and proposing a series of consensus statements, which were reviewed and approved by the NAIMS. In this review and consensus paper, we provide background on the use of 7T MRI in MS research, highlighting this technology's promise for identification and quantification of aspects of MS pathology that are more difficult to visualize with lower-field MRI, such as grey matter lesions, paramagnetic rim lesions, leptomeningeal enhancement and the central vein sign. We also review the promise of 7T MRI to study metabolic and functional changes to the brain in MS. The NAIMS provides a series of consensus statements regarding what is currently known about the use of 7T MRI in MS, and additional statements intended to provide guidance as to what work is necessary going forward to accelerate 7T MRI research in MS and translate this technology for use in clinical practice and clinical trials. This includes guidance on technical development, proposals for a universal acquisition protocol and suggestions for research geared towards assessing the utility of 7T MRI to improve MS diagnostics, prognostics and therapeutic efficacy monitoring. The NAIMS expects that this article will provide a roadmap for future use of 7T MRI in MS.

1 Department of Neurology, University of Maryland School of Medicine, Baltimore, MD 21201, USA
2 Department of Neurology, Baltimore VA Medical Center, Baltimore, MD 21201, USA
3 Neuroimaging Program, Department of Neurology, Cedars-Sinai Medical Center, Los Angeles, CA 90048, USA
4 Department of Neurology, Massachusetts General Hospital, Harvard Medical School, Boston, MA 02114, USA
5 McConnell Brain Imaging Centre, Montreal Neurological Institute-Hospital, Montreal, QC, Canada, H3A 2B4
6 Department of Neurology and Neurosurgery, McGill University, Montreal, QC, Canada, H3A 2B4
7 Neuroimaging Unit, Neuroimmunology Division, Department of Neurology, Vanderbilt University Medical Center, Nashville, TN 37212, USA
8 Department of Neurology, Nashville VA Medical Center, TN Valley Healthcare System, Nashville, TN 37212, USA
9 Department of Neurology, Icahn School of Medicine at Mount Sinai, New York, NY 10029, USA
10 Russell H. Morgan Department of Radiology and Radiological Science, The Johns Hopkins University School of Medicine, Baltimore, MD 21205, USA
11 Laboratory of Advanced Imaging in Neuroimmunological Diseases, Fundació de Recerca Clínic Barcelona-Institut

Received April 04, 2024. Revised August 28, 2024. Accepted October 07, 2024. Advance access publication October 9, 2024
Published by Oxford University Press on behalf of the Guarantors of Brain 2024.

d'Investigacions Biomèdiques August Pi i Sunyer (FRCB-IDIBAPS), Hospital Clinic Barcelona, 08036 Barcelona, Spain
12 Translational Imaging in Neurology (ThINk) Basel, Department of Biomedical Engineering, Faculty of Medicine, University Hospital Basel, University of Basel, 4001 Basel, Switzerland
13 Research Center for Clinical Neuroimmunology and Neuroscience Basel (RC2NB), University Hospital Basel, University of Basel, 4001 Basel, Switzerland
14 Department of Health Sciences, University of Genova, 16132 Genova, Italy
15 Translational Neuroradiology Section, National Institute of Neurological Disorders and Stroke, National Institutes of Health, Bethesda, MD 20892, USA
16 Advanced MRI Section, National Institutes of Health, Bethesda, MD 20892, USA
17 Department of Neurology, University Hospital Basel, 4001 Basel, Switzerland
18 Department of Neurology, UCSF Weill Institute for Neurosciences, University of California, San Francisco, CA 94158, USA
19 Department of Radiology, Athinoula A. Martinos Center for Biomedical Imaging, Massachusetts General Hospital, Harvard Medical School, Charlestown, MA 02114, USA
20 Department of Radiology and Biomedical Imaging, University of California San Francisco, San Francisco, CA 94158, USA
21 Mellen Center for Multiple Sclerosis, Neurological Institute, Cleveland Clinic, Cleveland, OH 44195, USA
22 Department of Biomedical Engineering, McGill University, Montreal, Quebec, Canada, H3A 2B4
23 Vanderbilt University Institute of Imaging Sciences, Vanderbilt University, Nashville, TN 37212, USA
24 Department of Radiology and Radiological Sciences, Vanderbilt University, Nashville, TN 37212, USA
25 Department of Biomedical Imaging and Image Guided Therapy, Medical University of Vienna, 1090 Vienna, Austria
26 Department of Neurology, Brigham and Women's Hospital, Harvard Medical School, Boston, MA 02115, USA
27 Department of Neurology, Weill Cornell Medicine, New York, NY 10065, USA
28 Radiology, Pathology and Laboratory Medicine, Physics and Astronomy, International Collaboration on Repair Discoveries, University of British Columbia, Vancouver, Canada, BC V6T 1Z4

Correspondence to: Daniel M. Harrison, MD, Department of Neurology, University of Maryland School of Medicine,
110 South Paca Street
3rd Floor, Baltimore, MD 21201, USA
E-mail: dharrison@som.umaryland.edu

Keywords: multiple sclerosis; magnetic resonance imaging; 7 Tesla; ultra-high field

Graphical Abstract

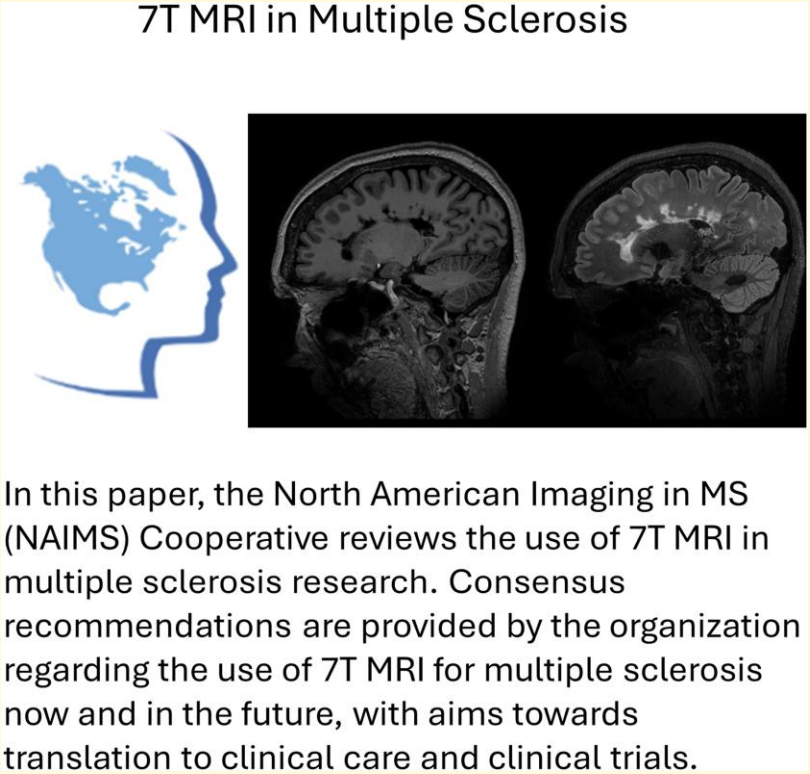

Introduction

From the earliest days of the use of ultra-high-field (UHF) MRI, particularly at 7 Tesla (7T), it has been clear that this technology holds promise to gain a greater understanding of multiple sclerosis (MS) pathology. The increased contrast, signal-to-noise ratio (SNR) and resolution made possible by combining 7T MRI with dedicated array detectors has allowed unprecedented spatial resolution[1,2] and enabled small and subtle cortical grey matter (GM) lesions in MS to be visualized.[2] The greater tissue contrast related to iron and myelin magnetic susceptibility effects at UHF immediately led to protocols for visualization of white matter lesions (WML) with central veins and chronic-active lesions with rims of iron-laden macrophages.[3-5] 7T protocols for identification MS pathology features that are very difficult to visualize using lower magnetic field strengths continue to improve over time and have also led to translation of some techniques to improve 3T MRI acquisitions. Despite the importance of high-field MRI work, UHF, and 7T MRI in particular, has remained a niche research tool for MS and has not yet been widely integrated into diagnostic methods or clinical workflows.

It is clear, however, that due to the maturation of the technology, recent regulatory approval and growing evidence of utility for the study of MS, the use of 7T MRI as both a research and clinical tool for MS is poised to rapidly expand. Year-by-year analysis of articles available on PubMed with the search terms of '7T' and 'multiple sclerosis' shows a doubling of the rate of publications on this topic over the past 10 years. Further, Food and Drug Administration (FDA) approvals in 2017 and 2020 resulted in the marketing of 7T MRIs as clinical devices in the USA by two manufacturers. Consequently, the number of centres with a 7T MRI device continues to increase, with currently > 100 7T MRI scanners worldwide (updated map kept by Laurentius Huber (NIH) found here), and some institutions have begun to integrate these scanners into clinical workflows.

Despite these advances, protocols that are standardized across sites for acquisition and analysis of 7T MRI for MS do not exist, nor has 7T MRI been validated as a tool for MS diagnosis or treatment effect monitoring. It is critical to undertake this effort now—before clinical-grade 7T MRI scanner usage is more widely implemented. Further, consensus on, and evidence for how to utilize 7T in MS may be a necessary pre-requisite for stakeholders (hospitals, radiology departments, insurance providers, etc.) to implement 7T MRI on a larger scale. For these reasons, the North American Imaging in Multiple Sclerosis (NAIMS) convened a workshop, gathering experts in the field, to review the status of 7T MRI in MS and to propose an agenda for implementation of 7T technology in a coherent manner for the greatest future impact. The following manuscript is documentation of this effort. This paper, and subsequent work emanating from it, will accelerate the pace of 7T research in MS and bring us closer to its integration into clinical trials and clinical practice.

Materials and methods

On 21 and 22 February 2023, the NAIMS held its annual workshop at the site of the annual meeting of the Americas Committee for Treatment and Research in MS (ACTRIMS) in San Diego, CA, USA. All NAIMS members were invited to attend a series of talks given by invited experts in the field of UHF imaging and MS, including members of NAIMS and outside speakers. The topics of discussion and speaker list were put together by the organizing committee for this workshop (D.M.H., C.L., S.A.S., S.N., P.S. and E.C.K.) and can be found on the NAIMS website (https://www.naimscooperative.org/naims-workshop).

Prior to and during the meeting, members of the organizing committee used information gathered from the presentations, existing literature and expert opinion to draft a series of proposed consensus statements pertinent to clinical translation of 7T MRI in MS. These proposed consensus statements were discussed and debated at an open forum among all workshop attendees on the second day of the workshop. The consensus statements were edited based on feedback during the workshop and then integrated into this manuscript. Each workshop presenter also drafted a summary statement of their topic and submitted these to the organizing committee. These summaries were combined and edited to form the literature review portion of this manuscript. Drafts of this manuscript were then critically reviewed, modified and approved by the organizing committee, invited speakers, workshop session moderators and the NAIMS Steering Committee.

Findings in MS on structural MRI scans at 7T

Paramagnetic rim lesions

One of the greatest advantages of UHF MRI imaging is the improved susceptibility and T_2* contrast offered by gradient-recalled echo (GRE)-based sequences. Understanding of this concept led to early attempts to characterize iron content in the brains of those with MS on 7T MRI. Observations from these studies revealed a subtype of WML with a peripheral rim exhibiting paramagnetic resonance frequency shifts and increased apparent transverse relaxation rate (R_2*), which directly correlated with histopathologic iron staining in autopsied MS brains.[4,6,7] Further autopsy work confirmed co-localization of these iron rims with CD68+ inflammatory cells, suggesting that the paramagnetic rim lesion (PRL) subtype is an imaging surrogate for chronic-active WMLs.[8,9] This lesion type is commonly visible on multiple image types derived from GRE acquisitions, including magnitude T_2*

images, R_2* maps, unwrapped/filtered phase and quantitative susceptibility mapping (QSM)—some examples of PRL are shown in Fig. 1. The NAIMS has recently published a consensus paper discussing the various methods for identification and quantification of PRL, including 7T MRI methods.[10] PRL quantification on 7T MRI has increased our understanding of the evolution of these lesions and their clinical relevance, including data showing that this lesion type slowly expands over time and is associated with a greater risk of long-term disability accumulation.[8,11,12]

The interest in PRL as a surrogate for chronic-active WML at 7T spurred the development of similar techniques at lower field[13,14] and allowed for the accumulation of larger amounts of longitudinal data confirming clinical relevance and evaluations of the utility of PRL as a diagnostic biomarker for MS.[11,15] The translation of 7T MRI findings of PRL to lower field has also prompted work to study PRLs in the setting of clinical trials.[16,17]

Most of the early literature on PRLs described visualization on UHF MRI systems.[4,6,13] Systematic comparisons between 7T and lower-field methods are limited,[10,14] and thus, strong conclusions cannot be drawn as to the differential sensitivity to PRLs on 7T versus lower-field MRI. However, although PRL can be visualized on lower-field MRI, the exquisite sensitivity of 7T MRI to susceptibility signal alterations suggests that if the number of 7T MRI scanners can be increased and their imaging protocols unified, 7T MRI methods may be the best means by which to further study this important lesion type. It is for this reason that the recent NAIMS consensus on imaging chronic-active lesions in MS recommends 7T MRI as a gold-standard technique for visualization of PRL.[10]

Central vein sign

The central vein sign (CVS) is an MRI biomarker that may improve the accuracy of MS diagnosis.[18] It consists of the presence of a vein that is located in the centre of a WML, as visualized on iron-sensitive sequences such as susceptibility-weighted or T_2* sequences (Fig. 1).[19] Due to the predominant perivenular distribution of MS plaques,[20] the CVS is a typical finding in MS.

UHF MRI studies have been pivotal in visualization of the CVS, confirming initial findings and significantly advancing the field.[3-5,21] Sensitivity to the CVS is maximized at 7T due to increased SNR, higher spatial resolution and enhanced susceptibility effects—all of which improve vein conspicuity and visibility.[22]

Many MS plaques at 7T exhibit the CVS,[5,23] with a similar prevalence across different clinical MS phenotypes.[23,24] Seminal 7T studies have shown the value of the CVS in differentiating MS from other conditions, including neuromyelitis optica spectrum disorder (NMOSD),[25] Susac syndrome[26] and small vessel disease.[27,28] In one 7T study, the differentiation specificity of WML in MS from vascular

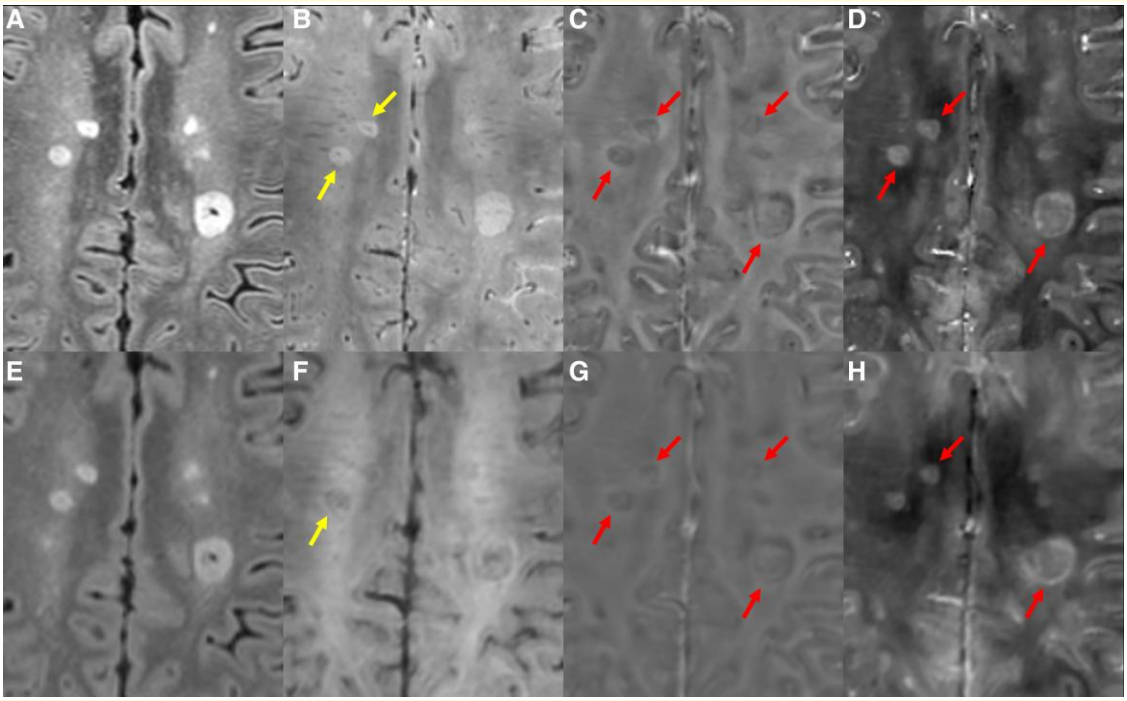

Figure 1 CVS and PRLs. 7T multi-echo 3D GRE (**A**), FLAIR (**B**), unwrapped phase (**C**) and QSM (**D**). Arrows in B indicate lesions with CVS visible on GRE. Arrows in C/D indicate PRL, seen as lesions with a hypointense rim on unwrapped phase and a hyperintense rim on QSM. 3T FLAIR (**E**), multi-echo GRE (**F**), unwrapped phase (**G**) and QSM (**H**) in the same person with MS. Although CVS and PRLs are visible, less detail can be seen on these images, leading to a reduced count of lesions marked as PRLs or having the CVS and less definitive and more subjective identification of both.

lesions was between 88 and 94% (depending on location) when accounting for the CVS, compared with between 63 and 69% without it.[29] Additionally, the CVS seen on 7T MRI proves valuable in predicting conversion to definite MS.[30]

Informed by the work done at 7T, modifications to lower-field MRI protocols provided improved diagnostic performance,[19,31-33] paving the way for vast applicability in the clinical setting. Nevertheless, the sensitivity for CVS detection is lower at 3 and 1.5T compared with 7T MRI. In a meta-analysis including 35 studies, the proportion of MS lesions with CVS was 82% at 7T, 74% at 3T and 58% at 1.5T.[31] The high sensitivity for CVS detection at 7T MRI is likely beneficial, especially for the assessment of challenging cases with small WML.[22]

The effect of MRI field strength on CVS prevalence needs to be considered when trying to define cut-offs for MS differential diagnosis in clinical practice. Additional factors can also influence the prevalence of CVS-positive lesions, including other technical factors (such as MRI protocols/post-processing tools)[19,34] and biological factors (including lesion topography[23,33] and the presence of vascular comorbidities[35]). Various criteria have been proposed for CVS-based thresholds for differentiating MS from other conditions.[19] The most frequently used are based on the proportion of the total lesions which exhibit the CVS;[19] notably, automated tools can significantly accelerate such assessment.[36,37] Other criteria suggest minimum CVS lesion count thresholds to ease clinical applicability.[38] Comparisons of these methods and potential integration into diagnostic criteria are being evaluated in ongoing trials—the data of which will be leveraged when implementing future decisions as to integration into clinical practice.[39]

Cortical and deep GM lesions

Cortical lesions (CLs) are common in MS, can be extensive and may arise via a somewhat distinct mechanism from WML.[40-45] Imaging CL *in vivo* is limited by their small size and the lower levels of myelin in normal cortex. Even advanced 1.5 and 3T methods have limited sensitivity for CL, especially for subpial lesions.[46-48] CLs are better seen with imaging contrasts sensitized to differences in either longitudinal or apparent transverse relaxation time constant (T_1 and T_2*, respectively). Such high-resolution T_1-weighted (T_1w) and T_2*w methods (Fig. 2) are sensitive to loss of myelin as well as loss of iron within CL, with the latter taking advantage of the increased susceptibility effects at 7T.[48-55]

High in-plane resolution T_2*w methods (<0.5 mm) have excellent CL contrast but require long acquisition times and are very sensitive to motion and B_0 inhomogeneity.[49] A high-resolution T_2*w method with navigator-based motion and B_0 correction has been developed but is not publicly available and requires off-scanner reconstruction.[56,57] Magnetization-prepared 2 rapid gradient echo (MP2RAGE), with its intrinsic correction for B_0 inhomogeneity and sensitivity to myelin, is the most widely used T_1w method for visualizing CLs at 7T and is typically employed with 0.7 mm^3 resolution.[51,58] The use of other high-resolution T_1w sequences is also reported,[52,59] including those with clinically feasible scan times. Increasing the resolution can improve CL visualization. One area of active research is the development of denoising and reconstruction algorithms, which may allow for improved SNR even at high resolution.[60]

Although more CLs are identified on high-resolution T_1w sequences than on T_2*w images,[51,59] subpial demyelination is often better seen on T_2*w images. A multi-contrast read that includes high-resolution MP2RAGE and T_2*w images leverages the advantages of each image type and allows confirmation of subtle lesions on two image types, potentially reducing false positives. However, there are limited data comparing visualization of CL with different 7T methods or different reading protocols, and the data that do exist are largely from small, single-centre cohorts.

Another limitation in the identification of CL is the time and expertise required to identify them, even on optimal images. Automated methods for CL detection have been proposed,[61,62] but require further testing and optimization using multi-centre data.

Despite the challenges of CL imaging, characterization of these lesions at 7T has confirmed their association with physical disability and cognitive dysfunction as well as with progressive disease.[49,52,63-65] One 7T longitudinal study suggested that, in contrast to WML formation, CL formation occurs at a higher rate in progressive than relapsing MS, raising the possibility that CL formation could underlie worsening disability in progressive MS.[64] CL burden may also be associated with subsequent worsening of disability.[64,66] The impact of current MS disease modifying therapies on CL is not known. The use of high-resolution images to analyse differences in CL appearance on T_1w versus T_2*w images as well as how CL morphology and signal intensity changes over time can potentially improve our understanding of the processes of CL formation and repair.

Lesions in deep GM or mixed GM/WM structures, such as the thalamus, may also benefit from UHF imaging (Fig. 3). Although not frequently described at 1.5 or 3T, multiple 7T studies have characterized and quantified lesion burden in the thalamus in MS and their potential clinical impact.[67-69] Similar to histopathology,[70,71] thalamic lesions appear to develop either as areas of widespread signal change in the subependymal region of the third ventricle or as ovoid shaped lesions in the body of the thalamus, typically centred on blood vessels. These lesions appear in 43–73% of people with MS scanned in 7T studies—more commonly so in those with progressive forms of MS and higher levels of disability.[67-69] Although some work suggests a close link between CL and thalamic lesion burden,[67] other data suggest that these lesion types may arise from separate pathologic mechanisms.[69,71] However, these conclusions are limited by small sample size studies and single-centre methodologies.

To advance the field of CL and deep GM lesion imaging, more feasible acquisition methods as well as automated segmentation methods are needed. In addition, larger,

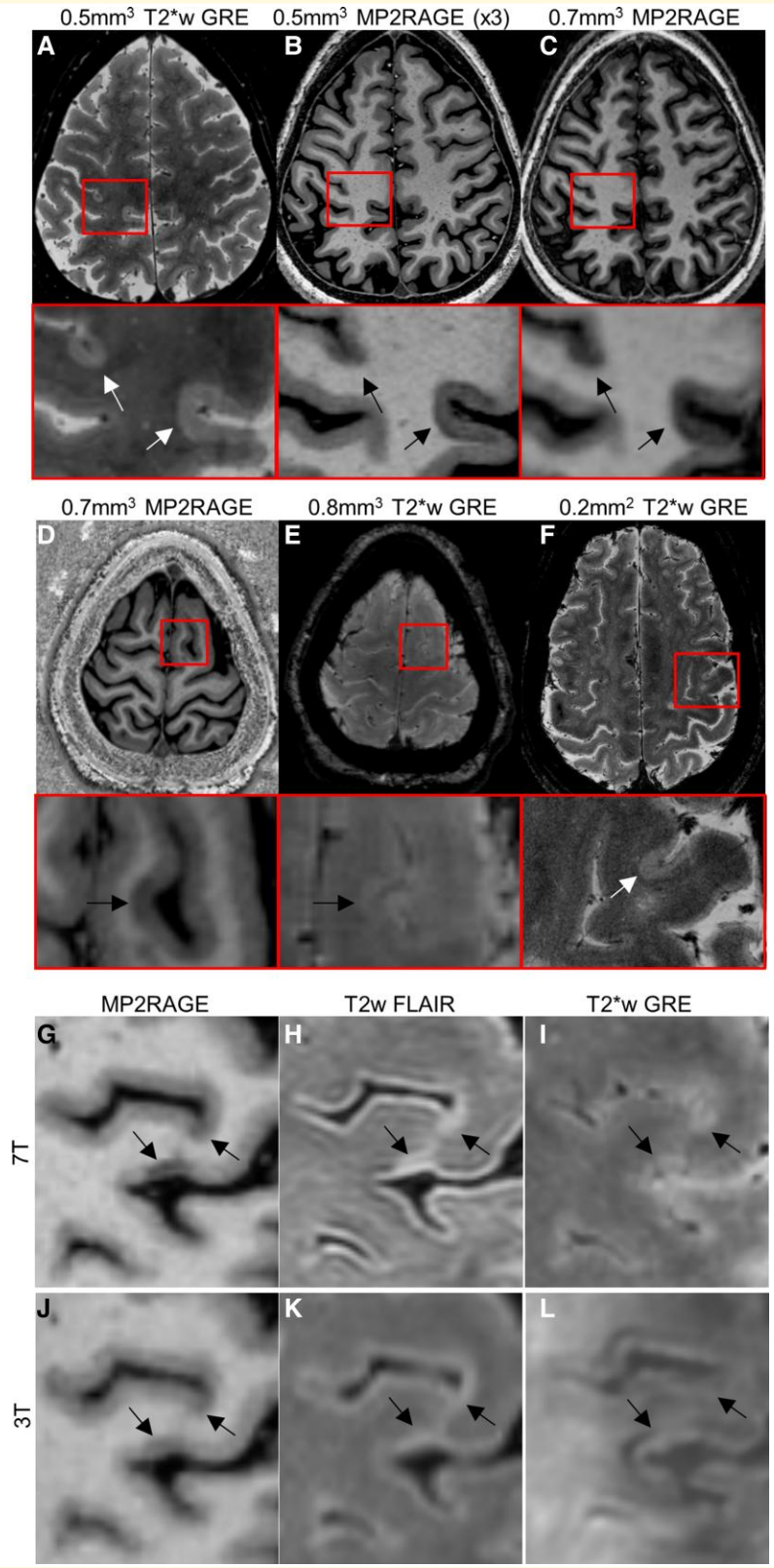

Figure 2 Cortical lesions. Two subpial lesions are well seen on a motion and B0-corrected, 3D 0.5-mm^3 T2*w GRE image (**A**, total acquisition time ~35 min. for three slabs covering the supratentorial brain) and on a median of 3 acquisitions of 0.5-mm^3. MP2RAGE (**B**, ~10 min/acquisition). Lesions are visible, but less well seen on a 0.7-mm^3. MP2RAGE image (acquisition time ~10 min). (**D**) and (**E**) A subpial lesion visualized on 0.7-mm^3 MP2RAGE but less well seen on a 0.8-mm^3 T2*w GRE image (acquisition time ~8 min). (**F**) A subpial lesion visualized on a 2D T2*w GRE image (0.2 mm^2 in-plane resolution, 1 mm slice thickness, ~24 min acquisition time for three slabs covering the supratentorial brain). Images in red boxes are magnifications of the regions outlined in red on whole-brain images above. A comparison of 7T (**G**–**I**) and 3T (**J**–**L**) images in the same MS subject. Arrows indicate locations of CLs as seen on MP2RAGE (**G**, **J**), FLAIR (**H**, **K**) and T2*w GRE (**I**, **L**).

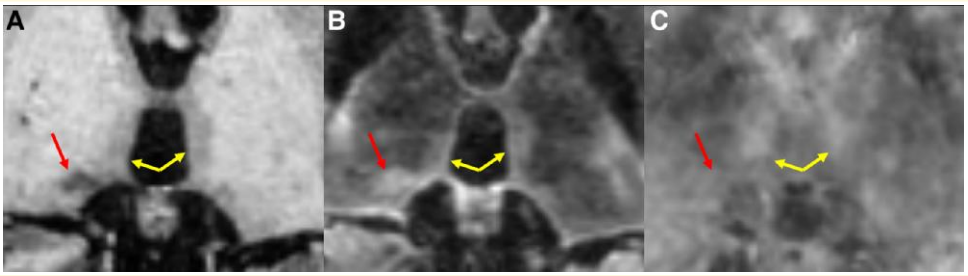

Figure 3 Thalamic lesions visualized on 7T MRI. Shown are MP2RAGE (**A**), FLAIR (**B**) and GRE (**C**). A thalamic body lesion is shown by the red arrow. Subependymal thalamic lesions are shown by the yellow arrows.

longitudinal and multi-centre studies are needed to better understand how CL and deep GM lesions form and how these lesions contribute, potentially independently, to disability. Finally, inclusion of 7T imaging into clinical trials in MS will be necessary to determine the effects of DMTs on CL and deep GM lesions.

Spinal cord lesions

Despite the clear importance of spinal cord (SC) pathology to MS-related disability, conventional SC MRI has not advanced to meet the demands for detecting subtle pathology in MS. 7T offers significant benefits to the SC imaging community through increased SNR and improved sensitivity to functional, vascular and structural changes that may occur in MS.

Although 7T imaging of the SC was first described in 2012,[72] techniques continue to be immature. A major factor in this regard is the limited availability of SC-dedicated MRI radiofrequency (RF) transmitters and detectors (also referred to as 'RF coils' or 'coils'), with only a small number of commercial coils available (each with their own limitations) and some 'in-house' coils built at various research institutions.[73] Additionally, there are several challenges to imaging the SC at any field strength, including a minimal GM/white matter (WM) and WM/WML difference in T_1 and T_2 relaxation times, temporal (respiration) and spatial (susceptibility) B_0 field inhomogeneity, motion and the small size of the internal structures. While 7T can worsen some of these challenges, the increased SNR alone leading to improved resolution and sensitivity to small lesions is potentially game changing. There are also several specific benefits of high-field SC MRI including (i) improved blood oxygenation dependent (BOLD) contrast for functional MRI studies, (ii) greater sensitivity to susceptibility (susceptibility-weighted MRI, SWI) and (iii) higher resolution for superior lesion detection. A recent study showed that more SC MS lesions can be detected at 7T than at 3T,[74] and in a small cohort, nearly every MS patient had lesions that could be detected at 7T.[75] These findings suggest that SC MRI at 7T could be useful for diagnostic evaluations in MS. 7T imaging of the SC could also be utilized to better probe the functional contribution of SC pathology to MS-related disability, as has been shown for techniques such as relaxometry,[76] diffusion,[77] chemical exchange saturation transfer[78] and resting-state functional connectivity.[79]

Future improvements of 7T SC imaging can be achieved by leaning on techniques and technologies that have been applied to anatomies such as the heart and other organs outside the CNS. The high-field SC MRI community remains small and contributions from investigators should be supported to increase awareness that improved SC imaging is necessary, and useful, but still understudied.

Meningeal enhancement

Histopathological work suggests that an interplay between inflammatory cell infiltrates in the meninges, meningeal lymphatic structures and meningeal vascular abnormalities likely contributes significantly to MS pathology.[80-84] Inflammatory cells trafficking through meningeal tissues and egressing to cervical lymph nodes may play a significant role in perpetuation of the inflammatory response in MS.[80,82] Further, ectopic lymphoid tissue development within meningeal tissues likely contributes to ongoing 'compartmentalized' inflammation in the CNS.[83-86] Because of the importance of meningeal tissues to the pathology of MS, much recent interest in neuroimaging has focused on the development of tools to measure these processes *in vivo*. Meningeal contrast enhancement (MCE) on post-contrast FLAIR MRI is a candidate biomarker for meningeal vascular and lymphatic pathology and function, and this technique has been applied to MS (Fig. 4). Specifically, leptomeningeal enhancement (LME) is described using post-contrast FLAIR MRI, and this finding can be associated with cortical GM atrophy and progressive MS phenotypes.[81,87] The use of 7T MRI may increase the sensitivity to LME.[88] A recent meta-analysis found that while 21% (95% CI 15–29%) of people with MS scanned using lower-field protocols had LME, 79% (95% CI 64–89%) had LME when scanned at 7T.[89] This increased sensitivity has been recently confirmed in a direct field comparison study.[88] The increased sensitivity of 7T MRI to both LME and CL may help confirm whether there is an association between meningeal inflammation and CL development—although preliminary work on this matter has led to conflicting findings.[58,68] Studies of ME at 7T also describe paravascular

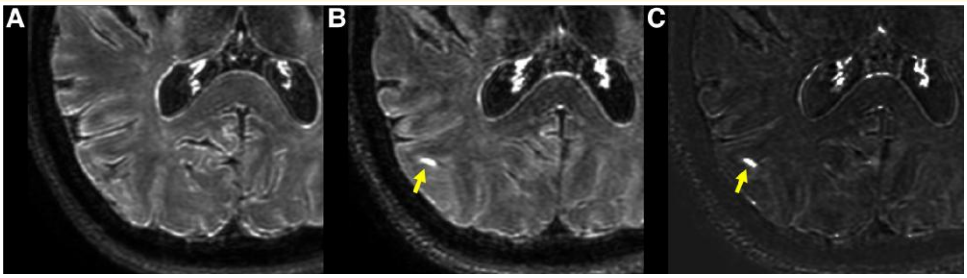

Figure 4 Leptomeningeal enhancement on 7T MRI. Shown is an example of LME (arrow). No enhancement seen in the same region on pre-Gd FLAIR (**A**), but a region of subarachnoid hyperintensity is seen on both Gd + FLAIR (**B**) and subtraction (Gd + minus Gd) (**C**).

and dural enhancement patterns that are stable over time,[90] and may represent gadolinium presence in lymphatic vessels[91,92]—suggesting that post-contrast 7T FLAIR may be suitable for mapping of the meningeal lymphatic network[93] and potentially indicate how it may be altered in human disease.

Consensus Statement #1	
Statement	The technical advantages of 7T MRI support improved sensitivity for visualization of certain findings in MS, including CVS, PRLs, cortical and deep GM lesions and LME.
Recommendation	Although most data suggest superiority of 7T MRI over lower field for visualization of CVS, PRLs, cortical and deep GM lesions and LME, more head-to-head studies are warranted, particularly in relationship to clinical relevance. In general, more studies evaluating 7T MRI as a diagnostic tool for MS should be performed, particularly in cases where it is difficult to make a diagnosis with lower field strengths.

Upon review of the data and findings presented in the prior sections using structural 7T MRI in MS, it is clear that 7T MRI provides a highly sensitive means by which to visualize CVS, PRLs, CL, deep GM lesions and LME—all in a manner that is advantageous over most lower-field MRI techniques. Similar superiority has not been established for typical WMLs. Larger head-to-head studies are necessary to compare CVS, PRLs, CL, deep GM lesions and LME from 7T MRI to lower field. If such work confirms the superiority of 7T MRI for each of these findings in MS, this will support the use of 7T MRI as a 'gold standard' for *in vivo* measurement of CVS, PRL, CL, deep GM lesions and LME in people with MS.

Data presented in the previous sections also suggest that 7T MRI techniques may aid in making accurate diagnoses of MS. The visualization of the CVS, PRLs, CL and deep GM lesions with high sensitivity and the typical lack of these findings in non-MS comparison groups support this conclusion. Future studies should target the use of multiple 7T MRI techniques for making an initial MS diagnosis directly compared to lower-field MRI in the same cohort.

Quantitative and functional MRI techniques at 7T in MS

Metabolic imaging

In vivo proton MR spectroscopy (MRS) of the human brain is a mature technique, first demonstrated in the 1980s. A number of brain metabolites can be detected at 1.5 or 3T, including *N*-acetyl aspartate (NAA, a marker of neuroaxonal health), creatine and phosphocreatine [total creatinine (tCr), energy metabolites], choline-containing compounds (tCho, membrane synthesis and degradation products), *myo*-inositol (mI, thought to be a glial cell marker) and glutamate and glutamine (Glx, compounds related to neurotransmission). In pathological states, lactate (Lac, the result of non-oxidative glycolysis) may also be detectable.[94]

Studies in people with MS in the 1990s showed that both active and chronic MS plaques had markedly different spectra from normal brain; changes included decreased NAA, as well as increased tCho, mI and Lac in active demyelination.[95,96] The related technique of MR spectroscopic imaging (MRSI) can map the distribution of these compounds at a spatial resolution of ≈1 cm^3[97] and often depicts metabolic abnormalities in MS 'normal-appearing white matter' (NAWM).[98] MRS studies in MS indicated several potential useful applications, including identification of early signs of demyelination in NAWM based on elevated ratios of tCho/tCr,[99] as well as measurement of axonal damage/disease burden based on global NAA/tCr measurements, the latter of which correlated well with measures of disability.[100]

MRS is a modality that benefits significantly as magnetic field strength increases; advantages include increased chemical shift dispersion and SNRs, and simplification of resonances from J-coupled moieties, which together allow for more compounds to be detected with higher precision. For instance, the ability to separately quantify glutamate and glutamine was found to be almost 4 times better at 7T than 3T; other compounds more readily detectable at 7T include the antioxidant glutathione.[101,102]

Recent MRSI studies at 7T demonstrated that metabolic images with nominal, isotropic spatial resolution as low as ≈3.3 mm (0.04 cm^3) can be achieved at 7T in scan times of

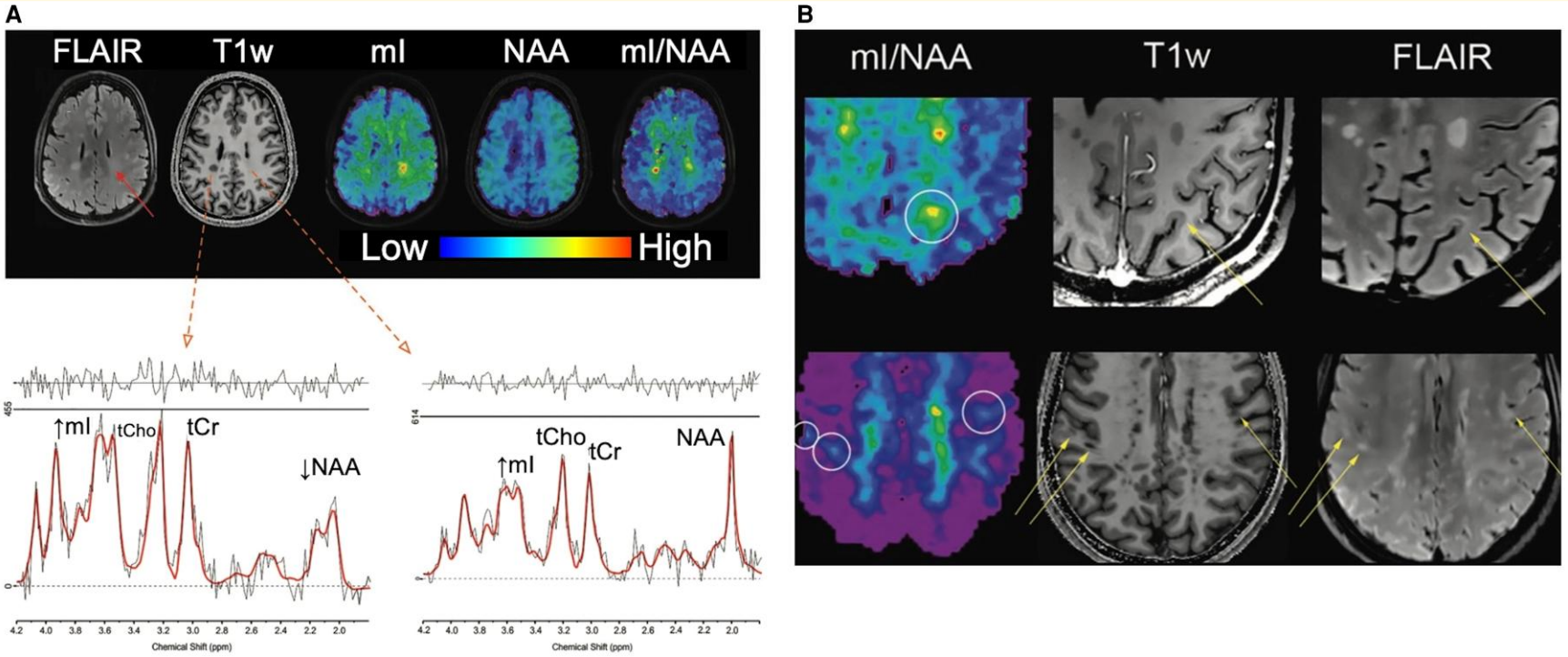

Figure 5 7T MRSI. 7T MRSI in (**A**) a patient with multiple sclerosis, showing conventional MRI, mI, NAA and mI/NAA ratio images. Spectra from the T_1-hypointense lesion in the right parietal white matter show decreased NAA and elevated tCho and mI. (**B**) mI/NAA and conventional MRI scans in two MS patients with cortical and sub-cortical lesions; mI/NAA maps depict these lesions clearly. Adapted with permission from Herckova *et al.* Radiology 2022;303(1):141–150.

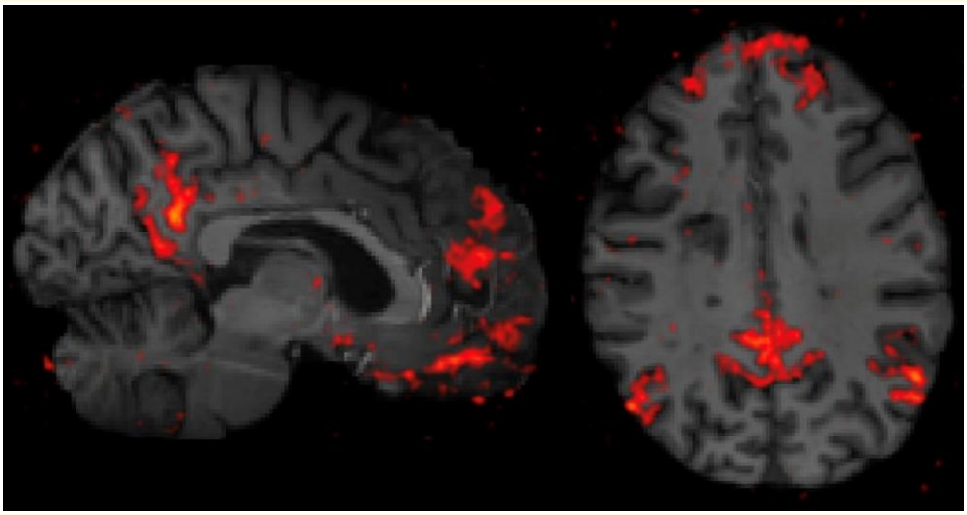

Figure 6 Resting-state functional connectivity at 7T. The bilateral posterior cingulate cortices were seeded to map the default mode network from a resting-state functional connectivity acquisition at 7T in an individual with multiple sclerosis. Sagittal (left) and axial (right) views demonstrate improved spatial resolution and spatial specificity to the cortex compared to capabilities at lower field strengths (not pictured).

the order of 20 min in a 3D axial slab with 50 mm coverage in the foot-head direction (Fig. 5).[103] This methodology is just starting to be applied to people with MS at 7T and has potential for visualizing abnormal WM, subtle cortical or subcortical pathology, as well as for evaluating disease burden.[104] The most relevant of these changes are a decrease of NAA and an increase of mI.[105] Mapping such changes could be developed into a marker for disease progression, as a correlation of 7T mI and NAA changes to EDSS disability scores early in the course of disease was recently demonstrated.[104]

In summary, 7T MRS and MRSI measure a 'panel' of brain compounds that inform on multiple aspects of brain metabolism, which are quantified with greater fidelity than at lower field. Therefore, MRS should be strongly considered for inclusion in 7T MR protocols of future studies in MS.

Functional MRI

Resting-state functional connectivity has been applied extensively to MS at 3T to evaluate brain connectivity and map distributed brain networks, with disease application to MS focusing on relating alterations in network properties to cognitive dysfunction.[106] The increased SNR that 7T affords can be leveraged to increase either the spatial or temporal resolution of the resting-state acquisition (example in Fig. 6), although technical tradeoffs of brain coverage and acquisition times exist.[107] Furthermore, seed-based analytical techniques demonstrate a higher spatial specificity to the cortex at 7T and improve network test-retest reliability.[108] While UHF resting-state studies in MS are currently limited, potential future applications of translating 3T resting-state studies to 7T could take advantage of improved spatial resolution to assess thalamic connectivity, hippocampal connectivity and laminar-based connectivity in the cortex—solidifying these mechanisms' role as biomarkers in MS.[109-112]

Multi-nuclear MRI

Non-proton-based magnetic resonance studies at 7T in MS are limited and could be a promising area for research. Sodium-23 (^{23}Na) gives the second strongest MR signal from biological tissue after ^{1}H and plays important roles in nerve signal transmission, axon integrity and cell function.[113,114] Due to its electric quadrupole moment (spin = 3/2), ^{23}Na experiences a strong interaction with local electric field gradients from the microscopic environment (nearby proteins), leading to fast biexponential T_2* decay.[115-117] Initially plagued by poor sensitivity and limited gradients at low field, higher field strength systems and new acquisition methods have improved ^{23}Na-MRI reliability.[118] Metrics that can be derived from ^{23}Na imaging include ^{23}Na concentration (total, intracellular and extracellular) and cellular volume fractions.[119,120] ^{23}Na relaxation and concentrations vary with CNS damage, suggesting that ^{23}Na-MRI may reveal features of tissue composition.[121] For example, additional sodium channels created after myelin loss in MS lead to increases in tissue sodium content,[122] and measures of cell volume fraction can indicate cellular swelling or cellular shrinkage/death. ^{23}Na 7T studies in MS are limited, but include demonstration of excellent scan-rescan reproducibility for measures of sodium concentration,[123] elucidation of differences between controls and SPMS WM but not GM[123] and the discovery that that total sodium concentration and intracellular sodium volume fraction correlate with lesion volumes and EDSS.[124] While ^{23}Na-MRI measures are not disease specific, ^{23}Na-MRI could potentially be useful for monitoring MS disease progression and treatment response.

Another non-proton nucleus relevant to MS disease processes is phosphorus-31 (^{31}P), the second most common nucleus for MRS studies. ^{31}P MRS studies can quantify chemicals related to phospholipid membrane composition, intra- and extracellular pH, magnesium (Mg) and energy

metabolism.[125,126] Multi-component T_2 of the ^{31}P broad component may reflect membrane rigidity and allow separation of bilayers from vesicles.[126] Metabolite levels, pH, Mg and T_2 vary with tissue changes, supporting the use of ^{31}P MR to probe microstructure.[127] Studies of ^{31}P at 7T in MS are not evident, but technical development and application efforts in this area are warranted.

Diffusion

Diffusion MRI is a powerful technique for probing tissue microstructure in the living human brain. UHF strengths at 7T and above boost the SNR of diffusion MRI, allowing for higher spatial resolution and more accurate and precise localization of tissue microstructure in the cortex and WM.[128,129] However, 7T MRI diffusion also has technical challenges that must be overcome.[128] Shorter T_2 and T_2* relaxation times at 7T lead to faster signal decays and image blurring. Susceptibility artefacts and distortions at 7T must also be addressed using advanced imaging and post-processing techniques. Finally, the increased transmit field inhomogeneity and RF power deposition at 7T can be exacerbated when using spin-echo (SE) encoding for diffusion MRI.[130]

Fortunately, many of the technical challenges that have traditionally limited applications of diffusion MRI at UHF have been addressed through various hardware and software advances, including simultaneous multi-slice or multi-band encoding,[131] segmented acquisitions and reduced field-of-view techniques.[132] Parallel transmit techniques improve the uniformity of excitation when pulse modifications are employed and enable greater slice acceleration to offer rapid acquisition of high-quality, high-resolution whole-brain diffusion MRI data.[133]

High-performance gradient technology originally pioneered as part of the Human Connectome Project[134]

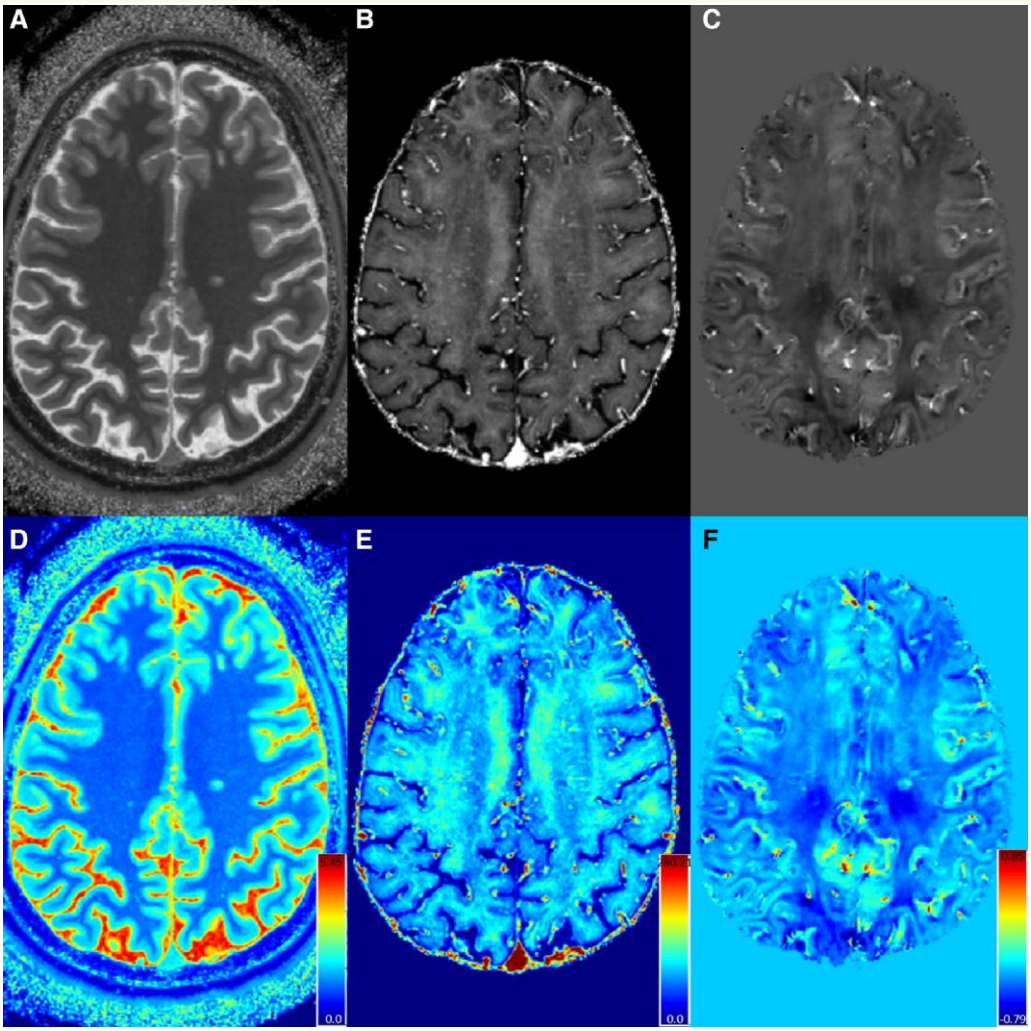

Figure 7 Quantitative maps from 7T MRI. Shown are a T_1 map (**A**, derived from MP2RAGE), R_2* map (**B**, derived from multi-echo GRE) and QSM (**C**, derived from multi-echo GRE). Each map is shown in colour scale below (**D**, **E**, **F**) with units of seconds for T_1 maps and milliseconds for R_2* and relative susceptibility (normalized to CSF) for QSM. Quantitation from these maps can be utilized for estimation of tissue myelin content, cell loss, etc.

provides significant benefits to diffusion MRI at 7T. Increasing the maximum gradient strength and slew rate of the gradients enable more efficient diffusion-encoding within shorter periods of time before significant signal decay occurs from T_2 shortening. Gradient amplitudes of up to 300 mT/m on the 3T Connectome MRI scanner[135] have been shown to sensitize the diffusion MRI measurement to a degree that allows mapping axon diameter and density in healthy individuals[136,137] and probing axonal damage in MS.[138,139] Recognition of the benefits of stronger, faster gradients for probing mesoscale features in the living human brain has driven recent efforts supported by the NIH BRAIN Initiative to push the limits of gradient technology for the next-generation 3T Connectome 2.0 scanner (featuring maximum gradient strength of 500 mT/m and slew rate of 600 T/m/s)[140] and 7T impulse gradient (featuring maximum gradient strength of 200 mT/m and slew rate of 900 T/m/s).[141] As high-performance gradient technology becomes embedded into the next generation of commercially available MRI scanners for clinical research, UHF diffusion MRI may advance our understanding of the microstructural changes occurring in MS and how they relate to the progression of cognitive dysfunction and disability.

Magnetic properties mapping

GRE-based acquisitions at 7T provide the opportunity for development of sensitive and high-resolution versions of multiple types of quantitative maps of tissue magnetic field properties. One example is quantitative susceptibility mapping (QSM). QSM is a post-processing method that seeks to measure the spatial distribution of magnetic susceptibility (χ) in an object.[142-144] Human tissues have a range of χ values, with soft tissue and bone being diamagnetic relative to water (χ in the range of 0 to −30 ppb) while other components, such as air and chelates of iron, are paramagnetic relative to water (χ ranging from ∼40 to 400 ppb).[145] QSM can be jointly applied with apparent transverse relaxation rate (R_2*) mapping to more thoroughly characterize myelin, iron and other lower-concentration metals in the human brain[146] Moreover, through the application of UHF MRI, tissue differences in R_2* maps and the local magnetic field shifts produced by such endogenous field perturbations from iron, calcium and myelin, are increased. For example, R_2*and QSM values in MS are affected by focal accumulation of iron and by transient demyelination and remyelination[147-150] These effects are accentuated when applying MRI with field strengths ≥ 7T.

Although highly desirable, it is often difficult to directly map changes in either R_2* or χ alone to alterations in iron and myelin that may be associated with MS pathology. Despite this ambiguity, the use of combined R_2* and χ values derived from multi-echo gradient echo MRI can provide differentially sensitive information to better understand the dynamic processes of iron deposition and/or changes in myelin in MS lesions.[150,151] Increases in myelin content (e.g. due to remyelination) negatively shift the absolute χ because myelin is diamagnetic, while increases in iron content positively shift χ because iron chelates are paramagnetic. Increases in myelin or iron both elevate the R_2* values in an MR imaging voxel because both result in increased dephasing of the MRI signal. Values of χ in MS WMLs often increase after initial lesion formation and gadolinium enhancement.[151] This effect continues up to 4 years after lesion formation and may be followed by a return to the magnetic susceptibility of surrounding NAWM.[152,153] Measurement of χ metrics derived from both QSM and R_2* maps at 7T MRI (Fig. 7) reveals alterations in WML that are associated with disability, confirming the clinical relevance of these techniques at 7T.[154,155]

The frequent use of the MP2RAGE technique at 7T also allows for evaluations of quantitative T_1 relaxation times via a T_1 map created during MP2RAGE processing (Fig. 7). High-resolution T_1 maps have been used at 7T to differentiate between lesions with pure demyelination versus those with evidence of remyelination, as confirmed on histopathology.[156] Alterations in T_1 maps at 7T also reveal significant changes in PRLs compared to non-PRL WML,[155] suggesting demyelination and cellular loss. Contrast-enhanced T_1 maps at 7T can be used to probe blood–brain barrier abnormalities in WMLs in MS.[155,157,158]

Consensus Statement #2	
Statement	The following 7T MRI sequences appear to have capabilities (*specific use in parentheses*) for both clinical care and research in MS: • MP2RAGE or ME-MPRAGE with B_1 correction (*atrophy, segmentation, white and GM lesions*) • 3D FLAIR (*WM and GM lesion identification and segmentation*) • Whole-brain 3D multi-echo, gradient echo (ME-GRE) [*PRL, CVS, quantitative mapping (i.e. R_2*, χ)*]. • 2D multi-slab SE or ME GRE (*GM lesions, CVS, PRL*)
Recommendation	Industry and academia should collaborate to standardize the above sequences, achieve clinically feasible scan times and provide streamlined post-processing in real time.

In reviewing the data presented on the use of both structural and quantitative 7T MRI techniques, in addition to considering the typical uses of MRI in MS, we suggest that acquisition of the above set of sequences in MS studies would provide a universal set of information applicable for most clinical and research questions. More importantly, such a protocol would have direct clinical applications, providing images useful for lesion identification, lesion and brain segmentation and some quantitative techniques. Standardization of such sequences across scanner types is necessary to achieve this goal, and we urge industry and academia to collaborate on such an endeavour. Further translation to clinical use will also require further image acquisition optimization, including the typical reductions in acquisition time necessary for clinical translation. Streamlining currently off-line post-processing requirements, such as phase unwrapping and QSM processing, to real time is also necessary.

Table 1 Guidance to key literature on the use of various sequences for detection of MS pathology at 7T

Imaging target	Data for target characterization	Key 7T references
PRL	T_2* magnitude R_2* map Unwrapped, filtered phase SWI QSM	• Bagnato F, *et al.* Brain 2011; 134:3602–3615[6] • Dal-Bianco A, *et al.* Acta Neuropathol 2017; 1par33:25–42[8] • Harrison DM, *et al.* AJNR Am J Neuroradiol 2016; 37:1447–53[154] • Absinta M, *et al.* JAMA Neurol 2019; 76: 1474–1483[11] • Absinta M, *et al.* JCI 2016; 126(7): 2597–2609[12] • Bagnato F, *et al.* Brain 2024;Jan16:awae013[10]
CVS	T_2* magnitude SWI FLAIR* FLAIR-SWI	• Tallantyre EC, *et al.* Neurology 2008;70:2076–2078[5] • Sinnecker T, *et al.* Neurology 2012;79:708–714[25] • Mistry N, *et al.* JAMA Neurol 2013; 70:623–628[30] • Sati P, *et al.* Nat Rev Neurol 2016; 12:714–722[19]
Cortical and deep GM lesions	T_2* magnitude MP2RAGE T_1-weighted	• Mainero C, *et al.*, Neurology, 2009; 73: 941–948[49] • Harrison DM, *et al.* Multiple Sclerosis; 21(9): 1139–1150.[67] • Harrison DM, *et al.* JAMA Neurol; 72(9): 1004–1012.[52] • Kilsdonk ID, *et al.* Brain 2016; 139:1472–1481[48] • Treaba CA, *et al.* Radiology 2019; 291:740–749[64] • Mehndiratta A, *et al.* Mult Scler 2021;27:674–683[69] • Beck ES, *et al.* Mult Scler 2022;28:1351–1363[65] • Beck ES *et al.*, Brain Commun 2024;6(3):fcae158[159]
Spinal cord lesions	T_2* magnitude T_2w-TSE MP2RAGE T_1-weighted ss-EPI	• Sigmund EE, *et al.* NMR Biomed 2012;25:891–899[72] • Dula AN, *et al.* Mult Scler 2016;22:320–328[74] • Massire A, *et al.* Neuroimage 2016;143:58–69[76] • Conrad BN, *et al.* Brain 2018;141:1650–1664[75] • Clarke MA, *et al.* Neuroimage 2023;284:120460[160]
Myelin	MP2RAGE T_1 map T_2, T_2* magnitude Diffusion MT MRS	• Barletta V *et al.*, Front Neurol 2021 Sept 3;12:714820[161] • Li X *et al.*, Neuroimage Clin 2015 Mar 4;7:709–14[162] • Maranzano J *et al.* AJNR Am J Neuroradiol 2019 Jul;40(7):1162–1169[54] • Klawiter EC *et al.*, Neuroimage 2011 Apr 15;55(4):1454–60[163]
Axon pathology	Diffusion MRS	• Schiavi S *et al.*, Brain 2021 Feb 12;144(1):213–223[164] • Tackley G *et al.*, Neuroimage 2021 Sep;238:118225.[165] • Wood ET *et al.*, NMR Biomed 2015 Aug;28(8):976–987[166] • Kolbe SC *et al.*, Neuroimage 2020 May 1;211:116609[167]
Leptomeningeal enhancement	Gadolinium-enhanced FLAIR	• Harrison DM *et al.*, J Neuroimaging 2017 Sep;27(5):461–468[168] • Ighani M *et al.*, Mult Scler 2020 Feb;26(2):165–176[58] • Zurawski J *et al.*, Mult Scler 2020 Feb;26(2):177–187[68] • Mizell R *et al.*, Mult Scler 2022 Mar;28(3):393–405[169] • Harrison DM *et al.*, PLoS One 2024 May;19(5):e0300298[88]
Brain and spinal cord connectivity	DWI SE EPI T_2*-weighted rsfMRI (3D multi-shot GRE) T_2*-weighted BOLD fMRI multi-slice EPI	• Mangeat G *et al.*, Hum Brain Mapp 2018 May;39(5):2133–2146[170] • Conrad BN *et al.*, Brain 2018 Jun 1;141(6):1650–1664[75] • Shi Z *et al.*, World J Urol 2021 Sep;39(9):3525–3531[75] • Nemani *et al.*, Med Phys 2021 Oct;48(10):5756–5764[108]

FLAIR, fluid-attenuated inversion recovery; TSE, turbo spin echo; MT, magnetization transfer; MRS, magnetization resonance spectroscopy.

The above-mentioned sequences are of course not the only sequences that are advantageous at 7T, and the protocol suggested in Consensus Statement #2 is a proposed basic universal protocol that could be added to specialized studies. The various sequences useful for visualization and quantification of MS pathology are listed in Table 1, with associated references.

Safety considerations and technical challenges

Safety

Although 7T MRI recently received approval for use in clinical care, several safety issues exist at this UHF strength.[171,172] Forces on metallic implants as well as RF power deposition are significantly increased at 7T.[171] Various strategies can be used to minimize forces and risk of accidents at 7T including the use of zone restrictions and standardized screening.[173] Given the shorter RF wavelength at 7T (~11 cm versus 26 cm at 3T and 52 cm at 1.5T), metallic implants, devices and foreign bodies can induce heating and cause thermal injury.[171] So far, only a few implant devices have been cleared by manufacturers as 'MR Conditional' for 7T MRI.[171,174,175] Other devices need to be tested before implanted people can undergo 7T imaging. Tissue heating, indirectly measured by specific absorption rate (SAR), should be carefully monitored and minimized by decreasing RF pulse amplitude, duration and/or frequency or using dielectric pads to homogenize the B_1 field.[176-178] This is particularly crucial for parallel transmit (pTx) imaging which has not yet received regulatory clearance for diagnostic imaging. Tissue and body heating is of particular importance for tolerance of these MRIs in the MS patient because of the Uhthoff phenomenon, so the

accumulated RF energy deposition over the entire exam [measured via the specific energy dose (SED) or specific absorption (SA)] may need to be monitored in concert with MRI manufacturer warnings and alerts. The SED of an exam may be reduced to avoid excessive elevation of the patient's core temperature or discomfort level by using shorter pulse sequences and/or reduced RF pulse strength.

There is no evidence indicating long-term negative effects from exposure to 7T magnetic fields.[179] However, people can experience transient bioeffects including vertigo, dizziness, false feelings of motion, nausea, nystagmus and electrogustatory effects, which are more common and more severe at 7T.[171] These effects may be mitigated by slowing the rate at which people enter and exit the scanner bore.[171]

Standardized safety guidelines and comprehensive implant testing specific to 7T need to be established to guide its safe use in the clinic. There are also no published studies investigating the safety of scanning pregnant women at 7T, and current FDA-approved 7T systems impose a lower weight limit of 30 kg, restricting its use in paediatric populations.[172] Therefore, it is the responsibility of the institution that uses a 7T MRI scanner to conduct adequate participant selection, perform risk/benefit analysis for the studied population and ensure participant safety both before and during the imaging process using existing expert recommendations.[172]

Technical challenges

Given the SAR constraints imposed at UHF strengths, it is challenging to perform SE imaging at 7T. While SE-based sequences are minimally affected by inhomogeneities related to the static B_0 field, the repetitive use of refocusing RF pulses induces high RF power deposition. Decreasing the number of slices or lengthening the repetition time (TR) can reduce SAR load, but this results in long acquisition times for whole-brain imaging. One potential solution is the use of simultaneous multi-slice (SMS) imaging to shorten the acquisitions. However, SMS increases high RF energy deposition and may rapidly exceed SAR safety limits at 7T. Another limitation of SE imaging at 7T is the modest GM–WM tissue contrast obtained with the T_2-FLAIR sequence, which may also affect WML detection. This is primarily caused by the increased T_1 relaxation times at 7T, which results in inadequate signal recovery for GM and WM brain tissues when using an inversion-time nulling of CSF signal. A workaround to this issue is to apply a magnetization-preparation pre-pulse that reduces the unwanted T_1 weighting, in combination with long echo-train lengths of variable flip angles that maintain SAR within the safety limits. This approach provides reasonable acquisition times varying from 5 to 13 min when using an isotropic resolution of 0.8 mm.[180,181]

One way to avoid high energy deposition at 7T is to use gradient-echo (GRE) imaging. Given the relatively low RF deposition and rapid scanning speed, RF-spoiled GRE sequences can provide submillimeter whole-brain imaging with high SNR and tissue contrast. T_1w images can be acquired with a 0.7-mm isotropic resolution at 7T in <6 min using standard a 3D MPRAGE sequence. However, these T_1w images will be affected by intensity inhomogeneities related to non-uniformity of B_1 field across the brain and caused by multi-source RF transmission. This issue can be mitigated in various ways including: the use of tailored adiabatic inversion pulses that are insensitive to transmit RF variations, the use of parallel transmission (pTx) or the use of proton-density-weighted images.[182] This last solution is the so-called MP2RAGE sequence that collects two 3D imaging volumes using different inversion times and combines these volumes to synthetically produce T_1w images that are almost entirely free of image intensity inhomogeneities.[183] However, MP2RAGE scans require about 10 min when acquired at 0.7 mm isotropic at 7T. Interestingly, the use of parallel imaging (PI) based on controlled aliasing 2D-CAIPIRINHA undersampling can shorten the scan time down to 4 min while maintaining image quality.[184] Another complementary approach is the use of the wave-CAIPI technique with 2D-CAIPIRINHA to create a staggered corkscrew k-space trajectory.[185] This new technique can achieve a 12-fold acceleration for MPRAGE scans and acquire 1-mm isotropic T_1w images in less than a minute at 7T.[186]

Another practical application of RF-spoiled GRE sequences at 7T is for magnetic susceptibility-based imaging (e.g. T_2*, SWI, phase, QSM). 2D multi-slice GRE sequences can acquire susceptibility-weighted images with very high in-plane image resolution (250–500 μm) and relatively thin slices (1 mm or less). The use of flip angles just below the Ernst angle reduces unwanted T_1 weighting and provides adequate T_2* weighting for WMLs when using an echo time similar to the T_2* relaxation times of WM tissues (20–35 ms at 7T). However, 2D multi-slice GRE scans are relatively slow for whole-brain imaging at 7T (due to long TR) and multi-echo 3D GRE scans are typically preferred, especially for performing T_2* relaxometry and QSM.[187] PI can be used to further accelerate these scans and achieve sub-millimeter isotropic image resolution of the entire brain. However, a significant SNR penalty occurs even at 7T when pushing the acceleration factor (R) beyond 4. More efficient k-space sampling techniques have been recently developed including the 3D multi-shot echo-planar imaging (EPI) sequence. Initially developed for fMRI studies at 7T,[188] 3D EPI sequences can provide high-resolution structural images of the whole brain in a few minutes.[189] The additional use of navigator echoes can help reduce image artefacts caused by B_0 variations and odd–even line discrepancies. High-quality, whole-brain susceptibility images can be obtained at 0.5-mm isotropic resolution in ~8 min at 7T. The use of the wave-CAIPI technique is also possible to obtain 1-mm isotropic whole-brain susceptibility images in <3 min.[185] Due to its lower image distortion and image blurring, wave-CAIPI is particularly favourable for 7T susceptibility imaging and could be integrated across multiple GRE sequences (including 3D EPI).

A general drawback of high-resolution T_2*w MRI is its sensitivity to motion artefacts. This issue, particularly important in clinical populations, is the result of the long scan times required for this application, combined with the high sensitivity of T_2*w imaging to motion-induced

B_0 field shifts. Active efforts employing motion-tracking devices and MRI-based navigator signals are underway to mitigate this issue.[190,191]

Hardware and associated software improvements are also necessary for clinical translation of 7T MRI techniques. Although not yet available clinically, recent developments in pTx technology have unlocked new solutions for controlling the RF fields and limit energy deposition while improving RF field homogeneity. These techniques substantially improve the uniformity and quality of whole-brain, 3D imaging, particularly for the 3D FLAIR sequence that is a cornerstone of MS imaging. It will be crucial to bring parallel transmission technology to the FDA-approved clinical mode of 7T scanners to fully realize the gains in image quality possible with 7T for the study of MS. This could alleviate poor visualization of the brain due to signal dropout on 7T MRI that can occur due to field inhomogeneity in regions such as the brainstem, cerebellum and anterior temporal lobes. Further, as discussed in the SC MRI imaging section, significant improvements in dedicated SC coils are necessary, including widespread use of standardized commercial coils that attain images akin to those attainable with custom coils used in specialized research institutions.

Consensus Statement #3	
Statement	Additional technical work is necessary to assess safety, minimize technical challenges and facilitate clinical translation of 7T MRI for MS.
Recommendation	Industry and academia should collaborate on hardware and software modifications including: • Hardware adapted to patient disability • Motion-correction techniques • Acceleration/denoising techniques • Image artefact (B_1/B_0-related) mitigation techniques • Standardized methods for use of dielectric padding, shimming techniques, multi-channel/parallel transmit coils, direct signal control • Automated quantification techniques (brain and lesion segmentation, inline MP2RAGE and T_2*/QSM reconstruction) • Hardware, sequences and coils development for 7T SC imaging • Streamlined post-processing in real time

After reviewing the presented data on safety and technical challenges, it is clear that although 7T MRI could be brought into use as a clinical tool, work is necessary to translate improvements that have been realized in specialized research laboratories to widespread use in clinical scanners. Both hardware and software modifications to the FDA-approved scanner platforms are necessary to truly unleash the potential of 7T MRI as a diagnostic and prognostic tool for MS.

Use of 7T MRI in clinical workflows and multi-centre studies

The next stage in the evolution of 7T MRI beyond a niche research tool for MS will be to move its use out of the laboratory and into clinical applications, such as clinical care and as an outcome measure in clinical trials. Recent FDA approval of 7T MRI scanners and the increasing volume of installations of these scanners at institutions throughout the world have made this transition increasingly feasible.

Clinical workflows

One potential model for how 7T MRI can be integrated into clinical care is the use of a 7T scanner by one of the NAIMS member sites, Brigham and Women's Hospital. At the Brigham and Women's Hospital, a 7T Siemens Magnetom Terra was approved for clinical use in the Fall of 2018. At the time of the writing of this manuscript, an imaging protocol is being used that runs in 53 min of table time and consists of core sagittal 3D-T_1 MP2RAGE and 3D-T_2 FLAIR sequences with 0.7 mm^3 voxels obtained pre- and post-gadolinium contrast, each ~8 min in duration. The post-contrast FLAIR sequence is obtained with a 10-minute delay to provide sensitivity for the detection of LME. T_2*w (single echo, gradient echo, 0.8 mm^3, used for CVS) and 3D-T_2w sequences are also obtained. The Brigham and Women's team have acquired ~900 scans in people with MS for clinical purposes to-date, each of which has been billed to patient insurance and is approved and reimbursed at similar rates as seen at 3T. The cost of 7T systems and upkeep is supported in part by a philanthropic donation to the hospital. Although this financial arrangement is unique, insights into the use of 7T MRI as a clinical tool are being gained. Clinical 7T scans are being ordered for various reasons, such as to confirm an MS diagnosis, establish a baseline for the patient's cortical and deep GM lesion load and to investigate a cause for disease progression that might have escaped detection at 3T. Brigham and Women's physicians in this consensus group note that when comparing serial 3T versus 7T scans in people with MS, it is common to find a higher lesion load at 7T, in particular for cortical GM lesions and the appearance of small new WMLs. The same physicians also note that 7T MRI has proven most useful to the clinical team in cases where non-specific or subtle WMLs are present on lower-field MRI of the brain and additional information is necessary to determine whether a patient does or does not fulfil diagnostic criteria. Challenges have included patient implants/hardware, claustrophobia and body habitus exceeding table or coil limitations. Approximately 15% of patients experience transient disequilibrium in the scanner, but this has not prevented scan completion.

The University of Minnesota has recently published their experience with integration of 7T MRI imaging into clinical workflows.[192] They propose a 54-min protocol that includes high-resolution T_1w MPRAGE, FLAIR, T_2*w and double inversion recovery images, along with post-contrast acquisitions. They report detection of GM and WML, along with differentiation of patients with MS from those with other disorders (such as NMOSD and MOG antibody disorder) by use of CVS. These experiences have been replicated at several other NAIMS member sites, demonstrating that routine clinical 7T scanning is feasible and has the potential to provide useful information for clinical management.

Multi-centre studies

The overwhelming majority of MS studies utilizing 7T MRI to date have been single-centre in nature, with relatively small sample sizes. Acquisition methods tend to be centre- and/or scanner-specific, and analysis methods are often customized to meet the specifications of a particular scanner or laboratory. For this reason, it may be difficult to apply the conclusions drawn from these studies to the larger population of those with MS and may also provide obstacles for translation of methods for replication and implementation throughout the community. For these reasons, unified, multi-centre methods are necessary.

A few research groups have identified this need and have begun work to unify methods across sites and scanner manufacturers. The German Ultrahigh Field Imaging (GUFI) Cooperative, a group of multiple 7T MRI sites in Germany and Austria, have conducted a series of 'traveling head' studies, in which they performed testing of a common acquisition protocol on Siemens 7T MRI scanners of various configurations.[193,194] This work has shown the necessity of B_1 mapping for scanner calibration and second order B_0 shimming—all of which were necessary to attain images that were relatively homogeneous between sites. After modifying protocols for this purpose, the GUFI Cooperative demonstrated excellent coefficients of variation for segmented volumes and quantitative measures derived from sequences such as MP2RAGE and multi-echo GRE in supratentorial brain—although this was more limited in infratentorial brain. The UK7T network, made up of five sites in the UK, has also undertaken a similar goal, attempting to harmonize protocols that include both Siemens and Philips scanners of various configurations.[195] Their work supported the need for significant attention paid to harmonization of acquisition parameters, reconstruction methods for accelerated imaging and correction methods for B_1 and B_0 maps and EPI distortion. With such modifications, they were able to attain images at each site with no statistical inter- or intra-site differences for cortical thickness, quantitative metrics such as R_2* and magnetic susceptibility, SNR and BOLD activation signal.

The subjective experience of persons in UHF scanners has also been assessed on a multi-centre basis. A post-MRI survey of participants in 7 and 9.4T MRI studies in Germany showed that although reports of discomfort or abnormal sensations in the scanner are commonly reported, only 0.9% of scans needed to be aborted.[196]

The NAIMS has also attempted to address the need for unified multi-centre methods for 7T MRI, with five member sites currently collaborating on an NIH-funded study performing retrospective pooling of scans from their respective 7T studies in MS for a collaborative analysis of CLs, lesions in deep GM, PRLs and LME.

Consensus Statement #4	
Statement	Conclusions drawn from current 7T MRI studies in MS may be limited by small sample sizes and single-site scanner/protocol specifics and analysis methods.
Recommendation	Multi-site, harmonized data acquisition and analysis methods are necessary. This should include standardization of calibration, acquisition and reconstruction, quality assurance and analysis methods.

Although the data presented on the use of 7T MRI for visualization of MS pathology are compelling, most of these studies have sample sizes <50 and utilize methods of acquisition and analysis that are exclusive to the site of study. Work such as that being performed by GUFI, the UK7T Network and NAIMS 7T Working Group should be extended to develop and validate MS-specific acquisition and analysis techniques and that prior data from single-centre 7T studies in MS be replicated in larger sample size, multi-centre cohorts.

Consensus Statement #5	
Statement	Standardized and validated 7T MRI could provide a means by which to evaluate the effect of therapeutics on MS pathology best viewed using UHF in early phase clinical trials.
Recommendation	The research community and industry should collaborate on the establishment and validation of 7T MRI networks for therapeutic trials in MS.

Multi-centre validation work will provide an opportunity for the development of multi-centre networks, which would then be poised for use in early phase clinical trials. This would be of greatest utility in trials of medications that are hypothesized to affect MS pathology best viewed at 7T, such as chronic-active WMLs and cortical/deep GM lesion development. Utilization of such a network of 7T scanners could rapidly accelerate the development of novel therapeutics for MS.

Conclusion

The NAIMS strongly endorses further work to probe MS pathology with 7T MRI methods, in addition to translation of 7T MRI methods into clinical practice and for use as an outcome measure in clinical trials. Despite remaining technical challenges, 7T MRI has unique abilities to evaluate

aspects of MS that are very difficult to study at 1.5 or 3T. The promise of 7T MRI should not be ignored and NAIMS encourages academia and industry to directly collaborate to work to improve and standardize 7T techniques and hardware, potentially ushering in a whole new era of MS research, monitoring and management.

Acknowledgements

The authors wish to acknowledge the significant contribution of Karie Krantz, Association Manager for the NAIMS Cooperative. Karie's work to prepare for and implement the logistics of the annual workshop was critical to the success of this programme. The authors also wish to thank Nancy Sicotte and Lazar Fleysher, who participated in the workshop, but did not contribute to this paper, and Laurentius Huber (NIH) for providing information on the current distribution of 7T MRI scanners worldwide.

Funding

D.M.H. was supported by the National Institute of Neurological Disorders and Stroke R01NS122980 and R01NS104403, the National Multiple Sclerosis Society RG-2110-38460 and the United States Department of Defense MS210103. F.B. was supported by the National Multiple Sclerosis Society (RG-1901-33190), the National Institutes of Health (R21 NS116434-01A1), the U.S. Department of Veteran's Affairs (I01CX002160-01A1) and the Voros Innovation Impact Funds. P.S. was supported by the National Multiple Sclerosis Society RG-2110-38526. S.N. was supported by the Canadian Institutes of Health Research FRN PJT-153005. S.G. was supported by the National Multiple Sclerosis Society RFA-2203-39369, the National Institute of Neurological Disorders and Stroke R01NS104283 and the National Institute of Neurological Disorders and Stroke R01105144. S.A.S. was supported by the National Institute of Neurological Disorders and Stroke R01NS117816 and the National Institute of Neurological Disorders and Stroke R01NS109114. E.S.B. was supported by the National Multiple Sclerosis Society (TA-2109-38412). J.D. was supported by the National Institute of Neurological Disorders and Stroke. M.D. was supported by the Intramural Research Program of National Institute of Neurological Disorders and Stroke (Z01NS0003119) and the Adelson Medical Research Foundation. A.C. was supported by the EUROSTARS E! 113682 HORIZON2020. S.Y.H. was supported by the National Institute of Biomedical Imaging and Bioengineering P41EB030006 and U01EB026996 and the National Institute of Neurological Disorders and Stroke R01NS118187. C.G. was supported by the Swiss National Science Foundation (SNSF) grant PP00P3_176984, Stiftung zur Förderung der gastroenterologischen und allgemeinen klinischen Forschung and the EUROSTARS E!113682 HORIZON2020. C.L. was supported by the Natural Sciences and Engineering Research Council of Canada, the International Collaboration on Repair Discoveries and the Craig H. Neilsen Foundation. A.C. was supported by the European Committe for Treatment and Research in Multiple Sclerosis (ECTRIMS) (2022), previously received a PhD studentship from the Multiple Sclerosis Society (UK) (2020) and is a Guarantors of Brain 'Entry' clinical fellowship (2019) and an European Committee for Treatment and Research in Multiple Sclerosis (ECTRIMS) —Magnetic Resonance Imaging in Multiple Sclerosis fellowship (2018). C.M. was supported by the National Institute of Neurological Disorders and Stroke 1R21NS1226737-01, the National Institute of Neurological Disorders and Stroke 1R21NS123419-01 and the United States Department of Defense MS210216.

Competing interests

D.M.H. has received research funding from EMD-Serono and Roche-Genentech, consulting fees from Horizon Therapeutics, TG Therapeutics and EMD-Serono and royalties from Up To Date, Inc. F.B. has received speaker honoraria from EMD-Serono, Sanofi and Novartis and serves/ed as site PI of multi-centre studies sponsored by EMD-Serono and Novartis and on advisory boards for Sanofi, EMD-Serono and Biogen. S.N. has received research funding from Roche-Genentech and Immunotec, consulting fees from Sana Biotechnology and personal compensation from NeuroRx Research. S.G. has received research funding from Roche-Genentech. E.S.B. has received consulting fees from EMD-Serono. .J.Z. has received research support from Novartis, I-Mab Biopharma and the Race to Erase MS Foundation. R.B. has received speaking honoraria from EMD-Serono and research support from Bristol-Myers Squibb, EMD-Serono and Novartis. A.C. was supported by the ECTRIMS post-doctoral training fellowship (2022). A.C. has received speaker honoraria from Novartis. S.Y.H. has received research funding and consulting fees from Siemens Healthineers. The University Hospital Basel (USB), as the employer of C.G., has received the following fees which were used exclusively for research support: (i) advisory board and consultancy fees from Actelion, Genzyme-Sanofi, Novartis, GeNeuro and Roche; (ii) speaker fees from Genzyme-Sanofi, Novartis, GeNeuro and Roche; and (iii) research support from Siemens, GeNeuro and Roche. E.C.K. has received research funding from Abbvie, Biogen and Genentech and consulting fees from EMD-Serono, Genentech, INmune Bio, Myrobalan Therapeutics, OM1, Inc. and TG Therapeutics. C.M. has received research funding from Genentech-Roche. C.L., J.D., M.D., D.A.R. and P.B. have no disclosures to report.

Data availability

Data sharing is not applicable to this article as no new data were created or analysed in this study.

References

1. Li TQ, van Gelderen P, Merkle H, Talagala L, Koretsky AP, Duyn J. Extensive heterogeneity in white matter intensity in high-resolution T2*-weighted MRI of the human brain at 7.0 T. *Neuroimage*. 2006;32:1032-1040.
2. Duyn JH, van Gelderen P, Li TQ, de Zwart JA, Koretsky AP, Fukunaga M. High-field MRI of brain cortical substructure based on signal phase. *Proc Natl Acad Sci U S A*. 2007;104:11796-11801.
3. Ge Y, Zohrabian VM, Grossman RI. Seven-Tesla magnetic resonance imaging: New vision of microvascular abnormalities in multiple sclerosis. *Arch Neurol*. 2008;65:812-816.
4. Hammond KE, Metcalf M, Carvajal L, *et al.* Quantitative in vivo magnetic resonance imaging of multiple sclerosis at 7 Tesla with sensitivity to iron. *Ann Neurol*. 2008;64:707-713.
5. Tallantyre EC, Brookes MJ, Dixon JE, Morgan PS, Evangelou N, Morris PG. Demonstrating the perivascular distribution of MS lesions in vivo with 7-Tesla MRI. *Neurology*. 2008;70:2076-2078.
6. Bagnato F, Hametner S, Yao B, *et al.* Tracking iron in multiple sclerosis: A combined imaging and histopathological study at 7 Tesla. *Brain*. 2011;134:3602-3615.
7. Yao B, Bagnato F, Matsuura E, *et al.* Chronic multiple sclerosis lesions: Characterization with high-field-strength MR imaging. *Radiology*. 2012;262:206-215.
8. Dal-Bianco A, Grabner G, Kronnerwetter C, *et al.* Slow expansion of multiple sclerosis iron rim lesions: Pathology and 7 T magnetic resonance imaging. *Acta Neuropathol.* 2017;133:25-42.
9. Absinta M, Maric D, Gharagozloo M, *et al.* A lymphocyte-microglia-astrocyte axis in chronic active multiple sclerosis. *Nature*. 2021;597:709-714.
10. Bagnato F, Sati P, Hemond CC, *et al.* Imaging chronic active lesions in multiple sclerosis: A consensus statement. *Brain*. 2024; 147:2913-2933.
11. Absinta M, Sati P, Masuzzo F, *et al.* Association of chronic active multiple sclerosis lesions with disability in vivo. *JAMA Neurol.* 2019;76:1474-1483.
12. Absinta M, Sati P, Schindler M, *et al.* Persistent 7-tesla phase rim predicts poor outcome in new multiple sclerosis patient lesions. *J Clin Invest*. 2016;126:2597-2609.
13. Haacke EM, Makki M, Ge Y, *et al.* Characterizing iron deposition in multiple sclerosis lesions using susceptibility weighted imaging. *J Magn Reson Imaging*. 2009;29:537-544.
14. Absinta M, Sati P, Fechner A, Schindler MK, Nair G, Reich DS. Identification of chronic active multiple sclerosis lesions on 3T MRI. *AJNR Am J Neuroradiol.* 2018;39:1233-1238.
15. Clarke MA, Pareto D, Pessini-Ferreira L, *et al.* Value of 3T susceptibility-weighted imaging in the diagnosis of multiple sclerosis. *AJNR Am J Neuroradiol.* 2020;41:1001-1008.
16. Calvi A, Clarke MA, Prados F, *et al.* Relationship between paramagnetic rim lesions and slowly expanding lesions in multiple sclerosis. *Mult Scler*. 2023;29:352-362.
17. Maggi P, Bulcke CV, Pedrini E, *et al.* B cell depletion therapy does not resolve chronic active multiple sclerosis lesions. *EBioMedicine*. 2023;94:104701.
18. Wattjes MP, Ciccarelli O, Reich DS, *et al.* 2021 MAGNIMS-CMSC-NAIMS consensus recommendations on the use of MRI in patients with multiple sclerosis. *Lancet Neurol.* 2021;20:653-670.
19. Sati P, Oh J, Constable RT, *et al.* The central vein sign and its clinical evaluation for the diagnosis of multiple sclerosis: A consensus statement from the North American Imaging in Multiple Sclerosis Cooperative. *Nat Rev Neurol.* 2016;12: 714-722.
20. Rae-Grant AD, Wong C, Bernatowicz R, Fox RJ. Observations on the brain vasculature in multiple sclerosis: A historical perspective. *Mult Scler Relat Disord*. 2014;3:156-162.
21. Duyn J, Koretsky AP. Magnetic resonance imaging of neural circuits. *Nat Clin Pract Cardiovasc Med*. 2008;5 Suppl 2: S71-S78.
22. Ineichen BV, Beck ES, Piccirelli M, Reich DS. New prospects for ultra-high-field magnetic resonance imaging in multiple sclerosis. *Invest Radiol*. 2021;56:773-784.
23. Kilsdonk ID, Lopez-Soriano A, Kuijer JP, *et al.* Morphological features of MS lesions on FLAIR* at 7 T and their relation to patient characteristics. *J Neurol*. 2014;261:1356-1364.
24. Kuchling J, Ramien C, Bozin I, *et al.* Identical lesion morphology in primary progressive and relapsing-remitting MS–an ultrahigh field MRI study. *Mult Scler*. 2014;20:1866-1871.
25. Sinnecker T, Dorr J, Pfueller CF, *et al.* Distinct lesion morphology at 7-T MRI differentiates neuromyelitis optica from multiple sclerosis. *Neurology*. 2012;79:708-714.
26. Wuerfel J, Sinnecker T, Ringelstein EB, *et al.* Lesion morphology at 7 Tesla MRI differentiates Susac syndrome from multiple sclerosis. *Mult Scler*. 2012;18:1592-1599.
27. Tallantyre EC, Dixon JE, Donaldson I, *et al.* Ultra-high-field imaging distinguishes MS lesions from asymptomatic white matter lesions. *Neurology*. 2011;76:534-539.
28. Mistry N, Abdel-Fahim R, Samaraweera A, *et al.* Imaging central veins in brain lesions with 3-T T2*-weighted magnetic resonance imaging differentiates multiple sclerosis from microangiopathic brain lesions. *Mult Scler*. 2016;22:1289-1296.
29. Kilsdonk ID, Wattjes MP, Lopez-Soriano A, *et al.* Improved differentiation between MS and vascular brain lesions using FLAIR* at 7 Tesla. *Eur Radiol*. 2014;24:841-849.
30. Mistry N, Dixon J, Tallantyre E, *et al.* Central veins in brain lesions visualized with high-field magnetic resonance imaging: A pathologically specific diagnostic biomarker for inflammatory demyelination in the brain. *JAMA Neurol*. 2013;70:623-628.
31. Castellaro M, Tamanti A, Pisani AI, Pizzini FB, Crescenzo F, Calabrese M. The use of the central vein sign in the diagnosis of multiple sclerosis: A systematic review and meta-analysis. *Diagnostics (Basel)*. 2020;10:1025.
32. Maggi P, Absinta M, Grammatico M, *et al.* Central vein sign differentiates multiple sclerosis from central nervous system inflammatory vasculopathies. *Ann Neurol*. 2018;83:283-294.
33. Sinnecker T, Clarke MA, Meier D, *et al.* Evaluation of the central vein sign as a diagnostic imaging biomarker in multiple sclerosis. *JAMA Neurol*. 2019;76:1446-1456.
34. Samaraweera AP, Clarke MA, Whitehead A, *et al.* The central vein sign in multiple sclerosis lesions is present irrespective of the T2* sequence at 3 T. *J Neuroimaging*. 2017;27:114-121.
35. Guisset F, Lolli V, Bugli C, *et al.* The central vein sign in multiple sclerosis patients with vascular comorbidities. *Mult Scler*. 2021; 27:1057-1065.
36. Dworkin JD, Sati P, Solomon A, *et al.* Automated integration of multimodal MRI for the probabilistic detection of the central vein sign in white matter lesions. *AJNR Am J Neuroradiol*. 2018;39:1806-1813.
37. Maggi P, Fartaria MJ, Jorge J, *et al.* CVSnet: A machine learning approach for automated central vein sign assessment in multiple sclerosis. *NMR Biomed*. 2020;33:e4283.
38. Solomon AJ, Watts R, Ontaneda D, Absinta M, Sati P, Reich DS. Diagnostic performance of central vein sign for multiple sclerosis with a simplified three-lesion algorithm. *Mult Scler*. 2018; 24:750-757.
39. Ontaneda D, Sati P, Raza P, *et al.* Central vein sign: A diagnostic biomarker in multiple sclerosis (CAVS-MS) study protocol for a prospective multicenter trial. *Neuroimage Clin*. 2021;32:102834.
40. Lucchinetti CF, Popescu BF, Bunyan RF, *et al.* Inflammatory cortical demyelination in early multiple sclerosis. *N Engl J Med*. 2011;365:2188-2197.
41. Bo L, Vedeler CA, Nyland HI, Trapp BD, Mork SJ. Subpial demyelination in the cerebral cortex of multiple sclerosis patients. *J Neuropathol Exp Neurol*. 2003;62:723-732.
42. Peterson JW, Bo L, Mork S, Chang A, Trapp BD. Transected neurites, apoptotic neurons, and reduced inflammation in cortical multiple sclerosis lesions. *Ann Neurol*. 2001;50:389-400.

43. Lagumersindez-Denis N, Wrzos C, Mack M, *et al.* Differential contribution of immune effector mechanisms to cortical demyelination in multiple sclerosis. *Acta Neuropathol*. 2017;134:15-34.
44. Albert M, Antel J, Bruck W, Stadelmann C. Extensive cortical remyelination in patients with chronic multiple sclerosis. *Brain Pathol*. 2007;17:129-138.
45. Strijbis EMM, Kooi EJ, van der Valk P, Geurts JJG. Cortical remyelination is heterogeneous in multiple sclerosis. *J Neuropathol Exp Neurol*. 2017;76:390-401.
46. Calabrese M, De Stefano N, Atzori M, *et al.* Detection of cortical inflammatory lesions by double inversion recovery magnetic resonance imaging in patients with multiple sclerosis. *Arch Neurol*. 2007;64:1416-1422.
47. Nelson F, Poonawalla AH, Hou P, Huang F, Wolinsky JS, Narayana PA. Improved identification of intracortical lesions in multiple sclerosis with phase-sensitive inversion recovery in combination with fast double inversion recovery MR imaging. *AJNR Am J Neuroradiol*. 2007;28:1645-1649.
48. Kilsdonk ID, Jonkman LE, Klaver R, *et al.* Increased cortical grey matter lesion detection in multiple sclerosis with 7 T MRI: A postmortem verification study. *Brain*. 2016;139:1472-1481.
49. Mainero C, Benner T, Radding A, *et al.* In vivo imaging of cortical pathology in multiple sclerosis using ultra-high field MRI. *Neurology*. 2009;73:941-948.
50. Nair G, Dodd S, Ha SK, Koretsky AP, Reich DS. Ex vivo MR microscopy of a human brain with multiple sclerosis: Visualizing individual cells in tissue using intrinsic iron. *Neuroimage*. 2020;223:117285.
51. Beck ES, Sati P, Sethi V, *et al.* Improved visualization of cortical lesions in multiple sclerosis using 7T MP2RAGE. *AJNR Am J Neuroradiol*. 2018;39:459-466.
52. Harrison DM, Roy S, Oh J, *et al.* Association of cortical lesion burden on 7-T magnetic resonance imaging with cognition and disability in multiple sclerosis. *JAMA Neurol*. 2015;72:1004-1012.
53. Beck ES, Gai N, Filippini S, Maranzano J, Nair G, Reich DS. Inversion recovery susceptibility weighted imaging with enhanced T2 weighting at 3 T improves visualization of subpial cortical multiple sclerosis lesions. *Invest Radiol*. 2020;55:727-735.
54. Maranzano J, Dadar M, Rudko DA, *et al.* Comparison of multiple sclerosis cortical lesion types detected by multicontrast 3T and 7T MRI. *AJNR Am J Neuroradiol*. 2019;40:1162-1169.
55. de Graaf WL, Kilsdonk ID, Lopez-Soriano A, *et al.* Clinical application of multi-contrast 7-T MR imaging in multiple sclerosis: Increased lesion detection compared to 3 T confined to grey matter. *Eur Radiol*. 2013;23:528-540.
56. Liu J, Beck ES, Filippini S, *et al.* Navigator-guided motion and B0 correction of T2*-weighted MRI improves multiple sclerosis cortical lesion detection. *Invest Radiol*. 2020;56:409-416.
57. Liu J, van Gelderen P, de Zwart JA, Duyn JH. Reducing motion sensitivity in 3D high-resolution T2*-weighted MRI by navigator-based motion and nonlinear magnetic field correction. *Neuroimage*. 2020;206:116332.
58. Ighani M, Jonas S, Izbudak I, *et al.* No association between cortical lesions and leptomeningeal enhancement on 7-Tesla MRI in multiple sclerosis. *Mult Scler*. 2019;26:165-176.
59. Cocozza S, Cosottini M, Signori A, *et al.* A clinically feasible 7-Tesla protocol for the identification of cortical lesions in multiple sclerosis. *Eur Radiol*. 2020;30:4586-4594.
60. Yu T, La Rosa F, Piredda GF, *et al.* Self-supervised image reconstruction of 7T MP2RAGE for multiple sclerosis: 0.5 mm isotropic resolution in 10 minutes. In: *International Magnetic Resonance in Medicine*. Annual Meeting (June 3–8, 2023), Toronto, ON, Canada. 2023.
61. Fartaria MJ, Sati P, Todea A, *et al.* Automated detection and segmentation of multiple sclerosis lesions using ultra-high-field MP2RAGE. *Invest Radiol*. 2019;54:356-364.
62. La Rosa F, Beck ES, Maranzano J, *et al.* Multiple sclerosis cortical lesion detection with deep learning at ultra-high-field MRI. *NMR Biomed*. 2022;35:e4730.
63. Nielsen AS, Kinkel RP, Madigan N, Tinelli E, Benner T, Mainero C. Contribution of cortical lesion subtypes at 7T MRI to physical and cognitive performance in MS. *Neurology*. 2013;81:641-649.
64. Treaba CA, Granberg TE, Sormani MP, *et al.* Longitudinal characterization of cortical lesion development and evolution in multiple sclerosis with 7.0-T MRI. *Radiology*. 2019;291:740-749.
65. Beck ES, Maranzano J, Luciano NJ, *et al.* Cortical lesion hotspots and association of subpial lesions with disability in multiple sclerosis. *Mult Scler*. 2022;28:1351-1363.
66. Treaba CA, Conti A, Klawiter EC, *et al.* Cortical and phase rim lesions on 7 T MRI as markers of multiple sclerosis disease progression. *Brain Commun*. 2021;3:fcab134.
67. Harrison DM, Oh J, Roy S, *et al.* Thalamic lesions in multiple sclerosis by 7T MRI: Clinical implications and relationship to cortical pathology. *Mult Scler*. 2015;21:1139-1150.
68. Zurawski J, Tauhid S, Chu R, *et al.* 7T MRI cerebral leptomeningeal enhancement is common in relapsing-remitting multiple sclerosis and is associated with cortical and thalamic lesions. *Mult Scler*. 2020;26:177-187.
69. Mehndiratta A, Treaba CA, Barletta V, *et al.* Characterization of thalamic lesions and their correlates in multiple sclerosis by ultra-high-field MRI. *Mult Scler*. 2021;27:674-683.
70. Vercellino M, Masera S, Lorenzatti M, *et al.* Demyelination, inflammation, and neurodegeneration in multiple sclerosis deep gray matter. *J Neuropathol Exp Neurol*. 2009;68:489-502.
71. Mahajan KR, Nakamura K, Cohen JA, Trapp BD, Ontaneda D. Intrinsic and extrinsic mechanisms of thalamic pathology in multiple sclerosis. *Ann Neurol*. 2020;88:81-92.
72. Sigmund EE, Suero GA, Hu C, *et al.* High-resolution human cervical spinal cord imaging at 7 T. *NMR Biomed*. 2012;25:891-899.
73. Barry RL, Vannesjo SJ, By S, Gore JC, Smith SA. Spinal cord MRI at 7T. *Neuroimage*. 2018;168:437-451.
74. Dula AN, Pawate S, Dortch RD, *et al.* Magnetic resonance imaging of the cervical spinal cord in multiple sclerosis at 7T. *Mult Scler*. 2016;22:320-328.
75. Conrad BN, Barry RL, Rogers BP, *et al.* Multiple sclerosis lesions affect intrinsic functional connectivity of the spinal cord. *Brain*. 2018;141:1650-1664.
76. Massire A, Taso M, Besson P, Guye M, Ranjeva JP, Callot V. High-resolution multi-parametric quantitative magnetic resonance imaging of the human cervical spinal cord at 7T. *Neuroimage*. 2016;143:58-69.
77. Massire A, Rasoanandrianina H, Taso M, *et al.* Feasibility of single-shot multi-level multi-angle diffusion tensor imaging of the human cervical spinal cord at 7T. *Magn Reson Med*. 2018;80:947-957.
78. Dula AN, Pawate S, Dethrage LM, *et al.* Chemical exchange saturation transfer of the cervical spinal cord at 7 T. *NMR Biomed*. 2016;29:1249-1257.
79. Barry RL, Smith SA, Dula AN, Gore JC. Resting state functional connectivity in the human spinal cord. *eLife*. 2014;3:e02812.
80. Louveau A, Herz J, Alme MN, *et al.* CNS lymphatic drainage and neuroinflammation are regulated by meningeal lymphatic vasculature. *Nat Neurosci*. 2018;21:1380-1391.
81. Absinta M, Vuolo L, Rao A, *et al.* Gadolinium-based MRI characterization of leptomeningeal inflammation in multiple sclerosis. *Neurology*. 2015;85:18-28.
82. Stern JN, Yaari G, Vander Heiden JA, *et al.* B cells populating the multiple sclerosis brain mature in the draining cervical lymph nodes. *Sci Transl Med*. 2014;6:248ra107.
83. Magliozzi R, Howell O, Vora A, *et al.* Meningeal B-cell follicles in secondary progressive multiple sclerosis associate with early

onset of disease and severe cortical pathology. *Brain*. 2007;130:1089-1104.
84. Magliozzi R, Howell OW, Reeves C, *et al.* A gradient of neuronal loss and meningeal inflammation in multiple sclerosis. *Ann Neurol*. 2010;68:477-493.
85. Choi SR, Howell OW, Carassiti D, *et al.* Meningeal inflammation plays a role in the pathology of primary progressive multiple sclerosis. *Brain*. 2012;135:2925-2937.
86. Magliozzi R, Howell OW, Nicholas R, *et al.* Inflammatory intrathecal profiles and cortical damage in multiple sclerosis. *Ann Neurol*. 2018;83:739-755.
87. Bergsland N, Ramasamy D, Tavazzi E, Hojnacki D, Weinstock-Guttman B, Zivadinov R. Leptomeningeal contrast enhancement is related to focal cortical thinning in relapsing-remitting multiple sclerosis: A cross-sectional MRI study. *AJNR Am J Neuroradiol*. 2019;40:620-625.
88. Harrison DM, Allette YM, Zeng Y, *et al.* Meningeal contrast enhancement in multiple sclerosis: Assessment of field strength, acquisition delay, and clinical relevance. *PLoS One*. 2024;19:e0300298.
89. Ineichen BV, Tsagkas C, Absinta M, Reich DS. Leptomeningeal enhancement in multiple sclerosis and other neurological diseases: A systematic review and meta-analysis. *Neuroimage Clin*. 2022;33:102939.
90. Jonas SN, Izbudak I, Frazier AA, Harrison DM. Longitudinal persistence of meningeal enhancement on postcontrast 7T 3D-FLAIR MRI in multiple sclerosis. *AJNR Am J Neuroradiol*. 2018;39:1799-1805.
91. Absinta M, Ha SK, Nair G, *et al.* Human and nonhuman primate meninges harbor lymphatic vessels that can be visualized noninvasively by MRI. *Elife*. 2017;6:e29738.
92. Ha SK, Nair G, Absinta M, Luciano NJ, Reich DS. Magnetic resonance imaging and histopathological visualization of human dural lymphatic vessels. *Bio Protoc*. 2018;8:e2819.
93. Patel LD, Raghavan P, Tang S, Choi S, Harrison DM. Imaging of the meningeal lymphatic network in healthy adults: A 7T MRI study. *J Neuroradiol*. 2023;50:369-376.
94. Oz G, Alger JR, Barker PB, *et al.* Clinical proton MR spectroscopy in central nervous system disorders. *Radiology*. 2014;270:658-679.
95. Koopmans RA, Li DK, Zhu G, Allen PS, Penn A, Paty DW. Magnetic resonance spectroscopy of multiple sclerosis: In-vivo detection of myelin breakdown products. *Lancet*. 1993;341:631-632.
96. Miller DH, Austin SJ, Connelly A, Youl BD, Gadian DG, McDonald WI. Proton magnetic resonance spectroscopy of an acute and chronic lesion in multiple sclerosis. *Lancet*. 1991;337:58-59.
97. Duyn JH, Gillen J, Sobering G, van Zijl PC, Moonen CT. Multisection proton MR spectroscopic imaging of the brain. *Radiology*. 1993;188:277-282.
98. Rooney WD, Goodkin DE, Schuff N, Meyerhoff DJ, Norman D, Weiner MW. 1H MRSI of normal appearing white matter in multiple sclerosis. *Mult Scler*. 1997;3:231-237.
99. Tartaglia MC, Narayanan S, De Stefano S, *et al.* Choline is increased in pre-lesional normal appearing white matter in multiple sclerosis. *J Neurol*. 2002;249:1382-1390.
100. De Stefano N, Narayanan S, Francis GS, *et al.* Evidence of axonal damage in the early stages of multiple sclerosis and its relevance to disability. *Arch Neurol*. 2001;58:65-70.
101. Mekle R, Mlynarik V, Gambarota G, Hergt M, Krueger G, Gruetter R. MR spectroscopy of the human brain with enhanced signal intensity at ultrashort echo times on a clinical platform at 3T and 7T. *Magn Reson Med*. 2009;61:1279-1285.
102. Tkac I, Oz G, Adriany G, Ugurbil K, Gruetter R. In vivo 1H NMR spectroscopy of the human brain at high magnetic fields: Metabolite quantification at 4T vs. 7T. *Magn Reson Med*. 2009;62:868-879.
103. Klauser A, Strasser B, Thapa B, Lazeyras F, Andronesi O. Achieving high-resolution (1)H-MRSI of the human brain with compressed-sensing and low-rank reconstruction at 7 tesla. *J Magn Reson*. 2021;331:107048.
104. Heckova E, Dal-Bianco A, Strasser B, *et al.* Extensive brain pathologic alterations detected with 7.0-T MR spectroscopic imaging associated with disability in multiple sclerosis. *Radiology*. 2022;303:141-150.
105. Lipka A, Niess E, Dal-Bianco A, *et al.* Lesion-specific metabolic alterations in relapsing-remitting multiple sclerosis via 7 T magnetic resonance spectroscopic imaging. *Invest Radiol*. 2023;58:156-165.
106. Jandric D, Lipp I, Paling D, *et al.* Mechanisms of network changes in cognitive impairment in multiple sclerosis. *Neurology*. 2021;97:e1886-e1897.
107. TV A, Jamison K, Glasser MF, *et al.* Tradeoffs in pushing the spatial resolution of fMRI for the 7T Human Connectome Project. *Neuroimage*. 2017;154:23-32.
108. Nemani A, Lowe MJ. Seed-based test-retest reliability of resting state functional magnetic resonance imaging at 3T and 7T. *Med Phys*. 2021;48:5756-5764.
109. Polimeni JR, Fischl B, Greve DN, Wald LL. Laminar analysis of 7T BOLD using an imposed spatial activation pattern in human V1. *Neuroimage*. 2010;52:1334-1346.
110. Deshpande G, Wang Y, Robinson J. Resting state fMRI connectivity is sensitive to laminar connectional architecture in the human brain. *Brain Inform*. 2022;9:2.
111. Ezama L, Hernandez-Cabrera JA, Seoane S, Pereda E, Janssen N. Functional connectivity of the hippocampus and its subfields in resting-state networks. *Eur J Neurosci*. 2021;53:3378-3393.
112. Chang WT, Langella SK, Tang Y, *et al.* Brainwide functional networks associated with anatomically- and functionally-defined hippocampal subfields using ultrahigh-resolution fMRI. *Sci Rep*. 2021;11:10835.
113. Madelin G, Lee JS, Regatte RR, Jerschow A. Sodium MRI: Methods and applications. *Prog Nucl Magn Reson Spectrosc*. 2014;79:14-47.
114. Allen P. *In vivo NMR spectroscopy*. Springer Verlag; 1990.
115. Zaric O, Juras V, Szomolanyi P, *et al.* Frontiers of sodium MRI revisited: From cartilage to brain imaging. *J Magn Reson Imaging*. 2021;54:58-75.
116. Bartha R, Menon RS. Long component time constant of 23Na T*2 relaxation in healthy human brain. *Magn Reson Med*. 2004;52:407-410.
117. Lommen JM, Flassbeck S, Behl NGR, *et al.* Probing the microscopic environment of (23) Na ions in brain tissue by MRI: On the accuracy of different sampling schemes for the determination of rapid, biexponential T2* decay at low signal-to-noise ratio. *Magn Reson Med*. 2018;80:571-584.
118. Meyer MM, Haneder S, Konstandin S, *et al.* Repeatability and reproducibility of cerebral (23)Na imaging in healthy subjects. *BMC Med Imaging*. 2019;19:26.
119. Madelin G, Kline R, Walvick R, Regatte RR. A method for estimating intracellular sodium concentration and extracellular volume fraction in brain in vivo using sodium magnetic resonance imaging. *Sci Rep*. 2014;4:4763.
120. Coste A, Boumezbeur F, Vignaud A, *et al.* Tissue sodium concentration and sodium T(1) mapping of the human brain at 3 T using a variable flip angle method. *Magn Reson Imaging*. 2019;58:116-124.
121. Huhn K, Engelhorn T, Linker RA, Nagel AM. Potential of sodium MRI as a biomarker for neurodegeneration and neuroinflammation in multiple sclerosis. *Front Neurol*. 2019;10:84.
122. Paling D, Solanky BS, Riemer F, *et al.* Sodium accumulation is associated with disability and a progressive course in multiple sclerosis. *Brain*. 2013;136:2305-2317.
123. Wilferth T, Mennecke A, Gast LV, *et al.* Quantitative 7T sodium magnetic resonance imaging of the human brain using a 32-channel phased-array head coil: Application to patients with secondary progressive multiple sclerosis. *NMR Biomed*. 2022;35:e4806.
124. Petracca M, Vancea RO, Fleysher L, Jonkman LE, Oesingmann N, Inglese M. Brain intra- and extracellular sodium concentration in multiple sclerosis: A 7 T MRI study. *Brain*. 2016;139:795-806.

125. Arias-Mendoza F, Brown TR. In vivo measurement of phosphorous markers of disease. *Dis Markers*. 2003;19:49-68.
126. Estilaei MR, Matson GB, Payne GS, Leach MO, Fein G, Meyerhoff DJ. Effects of chronic alcohol consumption on the broad phospholipid signal in human brain: An in vivo 31P MRS study. *Alcohol Clin Exp Res*. 2001;25:89-97.
127. Hnilicová P, Štrbák O, Kolisek M, *et al.* Current methods of magnetic resonance for noninvasive assessment of molecular aspects of pathoetiology in multiple sclerosis. *Int J Mol Sci*. 2020;22:21.
128. Gallichan D. Diffusion MRI of the human brain at ultra-high field (UHF): A review. *NeuroImage*. 2018;168:172-180.
129. Ugurbil K, Xu J, Auerbach EJ, *et al.* Pushing spatial and temporal resolution for functional and diffusion MRI in the Human Connectome Project. *NeuroImage*. 2013;80:80-104.
130. Wu X, Auerbach EJ, Vu AT, *et al.* High-resolution whole-brain diffusion MRI at 7T using radiofrequency parallel transmission. *Magn Reson Med*. 2018;80:1857-1870.
131. Setsompop K, Gagoski BA, Polimeni JR, Witzel T, Wedeen VJ, Wald LL. Blipped-controlled aliasing in parallel imaging for simultaneous multislice echo planar imaging with reduced g-factor penalty. *Magn Reson Med*. 2012;67:1210-1224.
132. Heidemann RM, Porter DA, Anwander A, *et al.* Diffusion imaging in humans at 7T using readout-segmented EPI and GRAPPA. *Magn Reson Med*. 2010;64:9-14.
133. Wu X, Schmitter S, Auerbach EJ, Ugurbil K, Van de Moortele PF. A generalized slab-wise framework for parallel transmit multiband RF pulse design. *Magn Reson Med*. 2016;75:1444-1456.
134. Setsompop K, Kimmlingen R, Eberlein E, *et al.* Pushing the limits of in vivo diffusion MRI for the Human Connectome Project. *NeuroImage*. 2013;80:220-233.
135. McNab JA, Edlow BL, Witzel T, *et al.* The Human Connectome Project and beyond: Initial applications of 300 mT/m gradients. *NeuroImage*. 2013;80:234-245.
136. Huang SY, Nummenmaa A, Witzel T, *et al.* The impact of gradient strength on in vivo diffusion MRI estimates of axon diameter. *NeuroImage*. 2015;106:464-472.
137. Huang SY, Tian Q, Fan Q, *et al.* High-gradient diffusion MRI reveals distinct estimates of axon diameter index within different white matter tracts in the in vivo human brain. *Brain Struct Funct*. 2020;225:1277-1291.
138. Huang SY, Fan Q, Machado N, *et al.* Corpus callosum axon diameter relates to cognitive impairment in multiple sclerosis. *Ann Clin Transl Neurol*. 2019;6:882-892.
139. Huang SY, Tobyne SM, Nummenmaa A, *et al.* Characterization of axonal disease in patients with multiple sclerosis using high-gradient-diffusion MR imaging. *Radiology*. 2016;280:244-251.
140. Huang SY, Witzel T, Keil B, *et al.* Connectome 2.0: Developing the next-generation ultra-high gradient strength human MRI scanner for bridging studies of the micro-, meso- and macro-connectome. *NeuroImage*. 2021;243:118530.
141. Vu A, Beckett A, Torrisi S, *et al.* Evaluation of high resolution diffusion MRI on the next-generation 7T scanner. In: *International Society for Magnetic Resonance in Medicine*. Annual Meeting (May 7-12, 2022) London, UK. 2022, p.5036.
142. de Rochefort L, Liu T, Kressler B, *et al.* Quantitative susceptibility map reconstruction from MR phase data using Bayesian regularization: Validation and application to brain imaging. *Magn Reson Med*. 2010;63:194-206.
143. Kressler B, de Rochefort L, Liu T, Spincemaille P, Jiang Q, Wang Y. Nonlinear regularization for per voxel estimation of magnetic susceptibility distributions from MRI field maps. *IEEE Trans Med Imaging*. 2010;29:273-281.
144. Schweser F, Deistung A, Lehr BW, Reichenbach JR. Quantitative imaging of intrinsic magnetic tissue properties using MRI signal phase: An approach to in vivo brain iron metabolism? *Neuroimage*. 2011;54:2789-2807.
145. Schenck JF. The role of magnetic susceptibility in magnetic resonance imaging: MRI magnetic compatibility of the first and second kinds. *Med Phys*. 1996;23:815-850.
146. Wang Y, Spincemaille P, Liu Z, *et al.* Clinical quantitative susceptibility mapping (QSM): Biometal imaging and its emerging roles in patient care. *J Magn Reson Imaging*. 2017;46:951-971.
147. Khalil M, Langkammer C, Ropele S, *et al.* Determinants of brain iron in multiple sclerosis: A quantitative 3T MRI study. *Neurology*. 2011;77:1691-1697.
148. Khalil M, Enzinger C, Langkammer C, *et al.* Quantitative assessment of brain iron by R(2)* relaxometry in patients with clinically isolated syndrome and relapsing-remitting multiple sclerosis. *Mult Scler*. 2009;15:1048-1054.
149. Elkady AM, Cobzas D, Sun H, Blevins G, Wilman AH. Progressive iron accumulation across multiple sclerosis phenotypes revealed by sparse classification of deep gray matter. *J Magn Reson Imaging*. 2017;46:1464-1473.
150. Rudko DA, Solovey I, Gati JS, Kremenchutzky M, Menon RS. Multiple sclerosis: Improved identification of disease-relevant changes in gray and white matter by using susceptibility-based MR imaging. *Radiology*. 2014;272:851-864.
151. Zhang Y, Gauthier SA, Gupta A, *et al.* Longitudinal change in magnetic susceptibility of new enhanced multiple sclerosis (MS) lesions measured on serial quantitative susceptibility mapping (QSM). *J Magn Reson Imaging*. 2016;44:426-432.
152. Chen W, Gauthier SA, Gupta A, *et al.* Quantitative susceptibility mapping of multiple sclerosis lesions at various ages. *Radiology*. 2014;271:183-192.
153. Dal-Bianco A, Grabner G, Kronnerwetter C, *et al.* Long-term evolution of multiple sclerosis iron rim lesions in 7 T MRI. *Brain*. 2021;144:833-847.
154. Harrison DM, Li X, Liu H, *et al.* Lesion heterogeneity on high-field susceptibility MRI is associated with multiple sclerosis severity. *AJNR Am J Neuroradiol*. 2016;37:1447-1453.
155. Choi S, Lake S, Harrison DM. Evaluation of the blood-brain barrier, demyelination, and neurodegeneration in paramagnetic rim lesions in multiple sclerosis on 7 tesla MRI. *J Magn Reson Imaging*. 2023;59:941-951.
156. Kolb H, Absinta M, Beck ES, *et al.* 7T MRI differentiates remyelinated from demyelinated multiple sclerosis lesions. *Ann Neurol*. 2021;90:612-626.
157. Choi S, Spini M, Hua J, Harrison DM. Blood-brain barrier breakdown in non-enhancing multiple sclerosis lesions detected by 7-Tesla MP2RAGE DeltaT1 mapping. *PLoS One*. 2021;16:e0249973.
158. van den Kerkhof M, Voorter PHM, Canjels LPW, *et al.* Time-efficient measurement of subtle blood-brain barrier leakage using a T1 mapping MRI protocol at 7 T. *Magn Reson Med*. 2021;85:2761-2770.
159. Beck ES, Mullins WA, Dos Santos Silva J, *et al.* Contribution of new and chronic cortical lesions to disability accrual in multiple sclerosis. *Brain Commun*. 2024;6:fcae158.
160. Clarke MA, Witt AA, Robison RK, *et al.* Cervical spinal cord susceptibility-weighted MRI at 7T: Application to multiple sclerosis. *Neuroimage*. 2023;284:120460.
161. Barletta V, Herranz E, Treaba CA, *et al.* Quantitative 7-Tesla imaging of cortical myelin changes in early multiple sclerosis. *Front Neurol*. 2021;12:714820.
162. Li X, van Gelderen P, Sati P, de Zwart JA, Reich DS, Duyn JH. Detection of demyelination in multiple sclerosis by analysis of [formula: See text] relaxation at 7 T. *Neuroimage Clin*. 2015;7:709-714.
163. Klawiter EC, Schmidt RE, Trinkaus K, *et al.* Radial diffusivity predicts demyelination in ex vivo multiple sclerosis spinal cords. *Neuroimage*. 2011;55:1454-1460.
164. Schiavi S, Petracca M, Sun P, *et al.* Non-invasive quantification of inflammation, axonal and myelin injury in multiple sclerosis. *Brain*. 2021;144:213-223.

165. Tackley G, Kong Y, Minne R, *et al.* An in-vivo 1H-MRS short-echo time technique at 7T: Quantification of metabolites in chronic multiple sclerosis and neuromyelitis optica brain lesions and normal appearing brain tissue. *Neuroimage*. 2021;238:118225.
166. Wood ET, Ronen I, Techawiboonwong A, *et al.* Investigating axonal damage in multiple sclerosis by diffusion tensor spectroscopy. *J Neurosci*. 2012;32:6665-6669.
167. Kolbe SC, Syeda W, Blunck Y, *et al.* Microstructural correlates of (23)Na relaxation in human brain at 7 Tesla. *Neuroimage*. 2020; 211:116609.
168. Harrison DM, Wang KY, Fiol J, *et al.* Leptomeningeal enhancement at 7T in multiple sclerosis: Frequency, morphology, and relationship to cortical volume. *J Neuroimaging*. 2017;27: 461-468.
169. Mizell R, Chen H, Lambe J, Saidha S, Harrison DM. Association of retinal atrophy with cortical lesions and leptomeningeal enhancement in multiple sclerosis on 7T MRI. *Mult Scler*. 2022; 28:393-405.
170. Mangeat G, Badji A, Ouellette R, *et al.* Changes in structural network are associated with cortical demyelination in early multiple sclerosis. *Hum Brain Mapp*. 2018;39:2133-2146.
171. Hoff MN, McKinney At, Shellock FG, *et al.* Safety considerations of 7-T MRI in clinical practice. *Radiology*. 2019;292:509-518.
172. Fagan AJ, Bitz AK, Bjorkman-Burtscher IM, *et al.* 7T MR safety. *J Magn Reson Imaging*. 2021;53:333-346.
173. ACR Committee on MR Safety; Greenberg TD, Hoff MN, *et al.* ACR guidance document on MR safe practices: Updates and critical information 2019. *J Magn Reson Imaging* 2020; 51: 331-338.
174. Feng DX, McCauley JP, Morgan-Curtis FK, *et al.* Evaluation of 39 medical implants at 7.0 T. *Br J Radiol*. 2015;88:20150633.
175. Shaffer A, Weisbaum D, Naik A, *et al.* Neurosurgical implant safety in 7 T MRI: A scoping review. *J Magn Reson Imaging*. 2023;57: 661-669.
176. Yang QX, Mao W, Wang J, *et al.* Manipulation of image intensity distribution at 7.0 T: Passive RF shimming and focusing with dielectric materials. *J Magn Reson Imaging*. 2006;24:197-202.
177. O'Brien KR, Magill AW, Delacoste J, *et al.* Dielectric pads and low- B1+ adiabatic pulses: Complementary techniques to optimize structural T1 w whole-brain MP2RAGE scans at 7 tesla. *J Magn Reson Imaging*. 2014;40:804-812.
178. Vaidya MV, Lazar M, Deniz CM, *et al.* Improved detection of fMRI activation in the cerebellum at 7T with dielectric pads extending the imaging region of a commercial head coil. *J Magn Reson Imaging*. 2018;48:431-440.
179. Fatahi M, Reddig A, Vijayalaxmi , *et al.* DNA double-strand breaks and micronuclei in human blood lymphocytes after repeated whole body exposures to 7T magnetic resonance imaging. *Neuroimage*. 2016;133:288-293.
180. Saranathan M, Tourdias T, Kerr AB, *et al.* Optimization of magnetization-prepared 3-dimensional fluid attenuated inversion recovery imaging for lesion detection at 7 T. *Invest Radiol*. 2014; 49:290-298.
181. Visser F, Zwanenburg JJ, Hoogduin JM, Luijten PR. High-resolution magnetization-prepared 3D-FLAIR imaging at 7.0 Tesla. *Magn Reson Med*. 2010;64:194-202.
182. Hurley AC, Al-Radaideh A, Bai L, *et al.* Tailored RF pulse for magnetization inversion at ultrahigh field. *Magn Reson Med*. 2010;63: 51-58.
183. Marques JP, Kober T, Krueger G, van der Zwaag W, Van de Moortele PF, Gruetter R. MP2RAGE, a self bias-field corrected sequence for improved segmentation and T1-mapping at high field. *Neuroimage*. 2010;49:1271-1281.
184. Shin W, Shin T, Oh SH, Lowe MJ. CNR improvement of MP2RAGE from slice encoding directional acceleration. *Magn Reson Imaging*. 2016;34:779-784.
185. Bilgic B, Gagoski BA, Cauley SF, *et al.* Wave-CAIPI for highly accelerated 3D imaging. *Magn Reson Med*. 2015;73:2152-2162.
186. Polak D, Setsompop K, Cauley SF, *et al.* Wave-CAIPI for highly accelerated MP-RAGE imaging. *Magn Reson Med*. 2018;79: 401-406.
187. QSM Consensus Organization Committee; Bilgic B, Costagli M, *et al.* Recommended implementation of quantitative susceptibility mapping for clinical research in the brain: A consensus of the ISMRM Electro-magnetic Tissue Properties Study group. *ArXiv* 2023.
188. Poser BA, Koopmans PJ, Witzel T, Wald LL, Barth M. Three dimensional echo-planar imaging at 7 Tesla. *Neuroimage*. 2010; 51:261-266.
189. Zwanenburg JJ, Versluis MJ, Luijten PR, Petridou N. Fast high resolution whole brain T2* weighted imaging using echo planar imaging at 7T. *Neuroimage*. 2011;56:1902-1907.
190. Polimeni JR, Bhat H, Witzel T, *et al.* Reducing sensitivity losses due to respiration and motion in accelerated echo planar imaging by reordering the autocalibration data acquisition. *Magn Reson Med*. 2016;75:665-679.
191. Liu J, van Gelderen P, de Zwart JA, Duyn JH. Reducing motion sensitivity in 3D high-resolution T(2)*-weighted MRI by navigator-based motion and nonlinear magnetic field correction. *Neuroimage*. 2020;206:116332.
192. Ozutemiz C, White M, Elvendahl W, *et al.* Use of a commercial 7-T MRI scanner for clinical brain imaging: Indications, protocols, challenges, and solutions—A single-center experience. *AJR Am J Roentgenol*. 2023;221:788-804.
193. Voelker MN, Kraff O, Brenner D, *et al.* The traveling heads: Multicenter brain imaging at 7 Tesla. *MAGMA*. 2016;29: 399-415.
194. Voelker MN, Kraff O, Goerke S, *et al.* The traveling heads 2.0: Multicenter reproducibility of quantitative imaging methods at 7 Tesla. *Neuroimage*. 2021;232:117910.
195. Clarke WT, Mougin O, Driver ID, *et al.* Multi-site harmonization of 7 tesla MRI neuroimaging protocols. *Neuroimage*. 2020;206:116335.
196. Rauschenberg J, Nagel AM, Ladd SC, *et al.* Multicenter study of subjective acceptance during magnetic resonance imaging at 7 and 9.4 T. *Invest Radiol*. 2014;49:249-259.